K

KOSTI

UNIVERSITI TEKNOLOGI MARA

Cawangan Pulau Pinang
Kampus Permatang Pauh

UiTM di hatiku

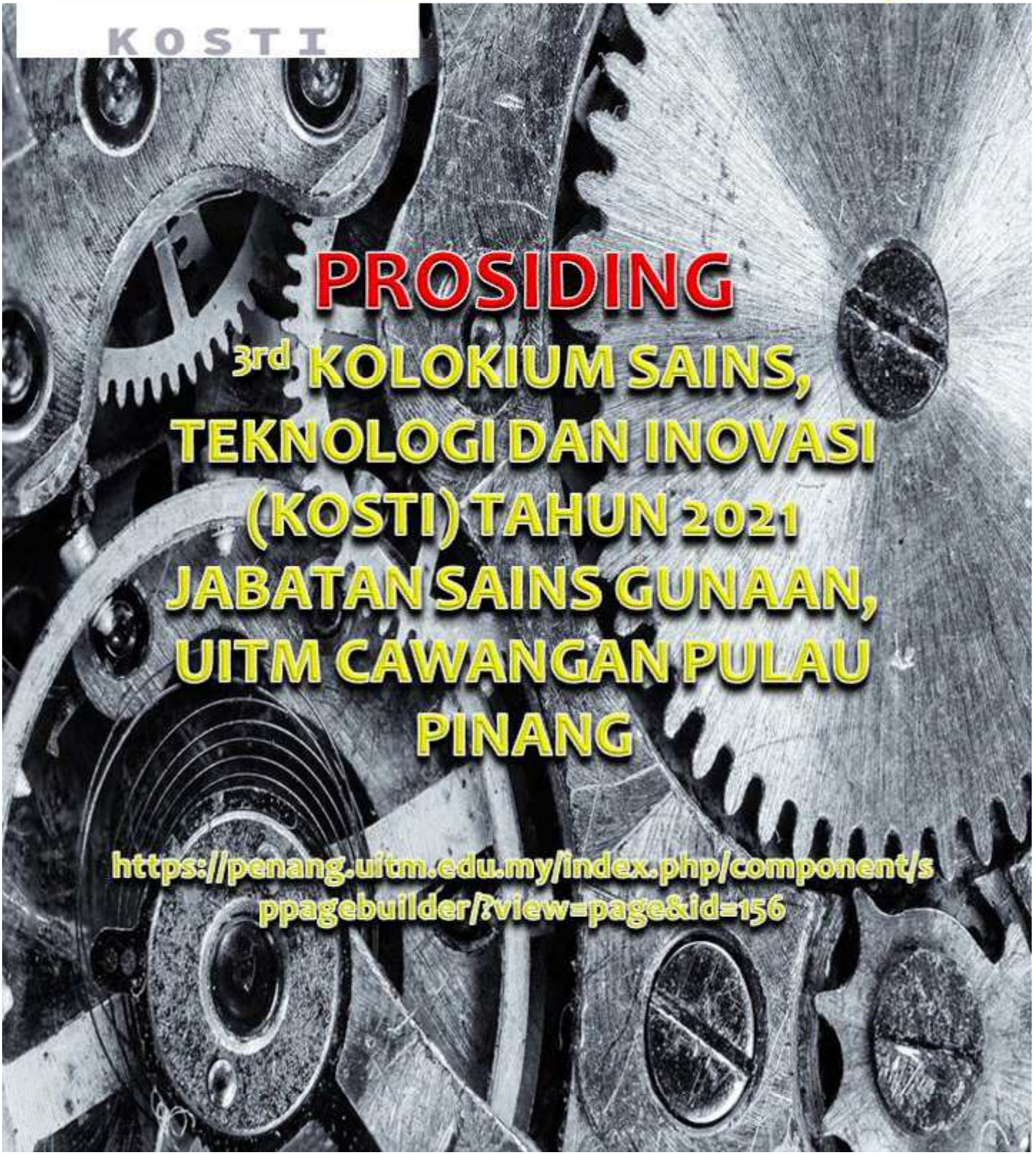

PROSIDING

3rd KOLOKIUM SAINS, TEKNOLOGI DAN INOVASI (KOSTI) TAHUN 2021

JABATAN SAINS GUNAAN, UITM CAWANGAN PULAU PINANG

https://penang.uitm.edu.my/index.php/component/sppagebuilder/?view=page&id=156

Imej Kulit: Pavlofox from Pixabay

e ISBN 978-967-26070-0-7

9 7 8 9 6 7 2 6 0 7 0 0 7

JABATAN SAINS GUNAAN
UNIVERSITI TEKNOLOGI MARA CAWANGAN PULAU PINANG
PENANG, MALAYSIA

DITERBITKAN PADA **30 SEPTEMBER 2021**

KANDUNGAN

PRAKATA

Alhamdulillah, puji syukur barisan penulis panjatkan kehadrat Allah SWT kerana atas berkat rahmat dan hidayah-Nya sehingga Prosiding 3rd Kolokium Sains, Teknologi dan Inovasi Tahun 2021, Jabatan Sains Gunaan, UiTM Cawangan Pulau Pinang dapat barisan penulis siapkan tepat pada waktunya.

Prosiding 3rd Kolokium Sains, Teknologi dan Inovasi Tahun 2021, Jabatan Sains Gunaan, UiTM Cawangan Pulau Pinang merupakan satu koleksi kajian penyelidikan yang telah berjaya dilaksanakan oleh barisan penulis dan penyelidik di Universiti Teknologi MARA, Cawangan Pulau Pinang. Hasil penyelidikan ini telah menyumbang banyak ilmu pengetahuan yang baru dan membuka peluang kerjasama diantara para penyelidik di UiTM Cawangan Pulau Pinang.

Penyelidikan yang dilakukan merentasi pelbagai bidang termasuk bidang sains, kejuruteraan dan inovasi. Hasil kajian ini telah dibentangkan kepada peserta-peserta kolokium dan hasil penulisan ini telah disemak oleh pensyarah di UiTM Cawangan Pulau Pinang.

Adalah diharapkan prosiding ini dapat memberi maklumat dan ilmu pengetahuan baru kepada pembaca dan seterusnya menjalinkan kerjasama di masa akan datang.

Sekian, Terima Kasih.

Mohd Zaki Mohd Yusoff
30 Sept 2021
Ketua Editor

COMPARATIVE STUDY ON TREATMENT OF WASTEWATER USING NATURAL AND CHEMICAL COAGULANT: A REVIEW

Randy Randock Anak Lawat[1], Nurul Izza Husin[2]*
[1]Faculty of Chemical Engineering, Universiti Teknologi MARA, Cawangan Pulau Pinang, 13500 Permatang Pauh, Pulau Pinang Malaysia
[2]Faculty of Applied Sciences, Universiti Teknologi MARA, Cawangan Pulau Pinang, 13500 Permatang Pauh, Pulau Pinang Malaysia
*corresponding author:nurulizza.husin@uitm.edu.my

ABSTRACT- The community are facing a serious issue regarding water scarcity due to the exponential population growth. In order to ensure sufficient water supply and meet the demand for clean water for sustainable development, various types of wastewater treatment technologies have been developed. Coagulation and flocculation processes are commonly used in a wide range of water treatment processes due to their simplicity and cost-effective approach. Chemical coagulants are commonly applied in the coagulation process for turbidity removal. However, it may lead to negative impacts on health issues. Therefore, natural coagulants are considered to be more environmentally friendly due to its biodegradability, renewability, non-toxicity and relative cost-effectiveness. This review paper aims to compare the effectiveness of natural coagulants and chemical coagulants, and to determine the best mixing conditions and settling time of coagulants. This paper highlights the effectiveness of natural and chemical coagulants applied in a different types of wastewater. The FTIR analysis proves the potential of natural coagulants in wastewater treatment due to the presence of functional groups such as carboxyl and hydroxyl group which could help in the coagulation process. Generally, each application of coagulants in a different type of wastewater has a different type of mixing conditions. Based on the evaluation, most of the optimum mixing condition is around 100-120 rpm. The settling time for coagulation and flocculation show variation due to the different types of coagulants and wastewater. In general, it shows that the turbidity removal increases as the settling time increases. Based on the review, it can be concluded the application of natural coagulants are feasible and reliable towards sustainable development.

Keywords: Wastewater. Natural coagulant, Settling time, Coagulation, Flocculation

1. INTRODUCTION

Wastewater refers to the effluent from a household, industries, commercial establishments and institutions, hospitals and others. It contains a high concentration of pollutants which may lead to negative impacts on the environment and human health. The rapid growth of urbanization activities influenced the generation of wastewater to be increased. Approximately, 80% of wastewater is discharged into waterways around the world. This action results in the existence of health, environmental and climate-related hazards [1]. Wastewater treatment is a crucial process to be considered as a significant aspect to sustain the environment, economy and society [2]. The

corresponding alternative for this issue is by recovering water, energy, nutrients, and other great value of material related to the wastewater field.

In general, there are three major stages involved in the wastewater treatment process which are primary treatment, secondary treatment and sludge treatment [3]. The selection of methods for wastewater treatment is depending on the quality of the wastewater. Proper treatment processes enhance the performance of the treatment to achieve high purification of water. Despite various wastewater treatment methods, coagulation and flocculation is the most relevant method because it is a low cost, simple and low energy consumption operation [4].

Coagulants exist in chemical-based and natural-based which are applied for the dissolve chemical species and turbidity removal in wastewater. Examples of chemical-based coagulants are polyaluminium chloride (PAC), aluminium sulphate (Alum) and ferric chloride ($FeCl_3$). While the natural-based coagulants such as cactus *Latifaria* and *Opuntia* [5]. The coagulant carries positively charged properties which will attract negatively charged particles of pollutants that exist in water which result from the colloidal particles neutralized to form suspended solids in the water [6].

However, the high cost and negative impact on human health and environmental factors of chemical-based coagulant indicate it is not compatible to apply in wastewater treatment [5]. On the other point, a natural coagulant is relatively cost-effective and has eco-friendly properties such as non-toxic, high biodegradability and non-corrosive [4].

2. RESEARCH METHODOLOGY

This review study was performed to collect articles in notable journals which provide crucial insights to researchers studying the comparative study on treatment of wastewater using natural and chemical coagulants. Wondimagegn Mengist et al presented a method to conduct a systematic literature review and meta-analysis studies for research [7]. This method consists of four basic steps as shown in Figure 1.

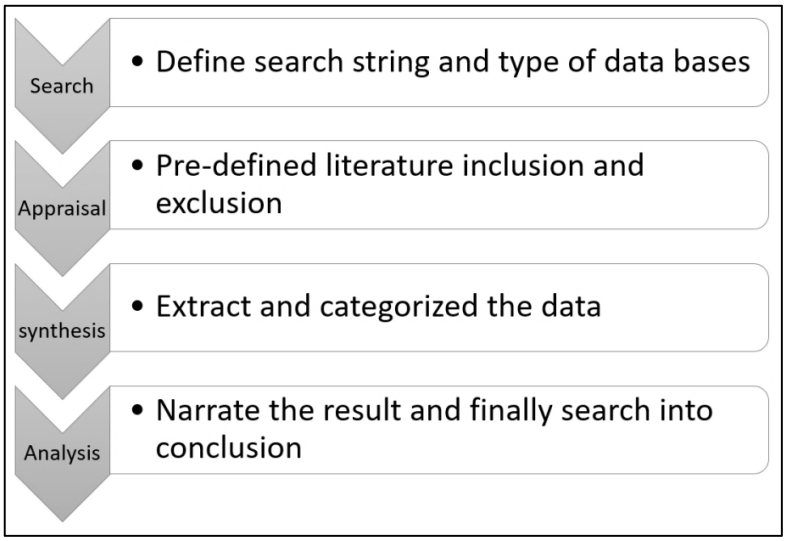

Figure 1: Research methodology basic steps flow chart.

There were a few main libraries database cover most of the papers while conducting this review such as ScienceDirect, ResearchGate, Springer and Google Scholar. The relevant papers were collected from significant databases with suitable hints (Treatment of wastewater AND coagulant; Treatment of wastewater AND natural coagulant AND chemical coagulant; Treatment of wastewater AND natural coagulant AND chemical coagulant AND coagulant mechanism; Treatment of wastewater AND natural coagulant AND chemical coagulant AND turbidity removal; Treatment of wastewater AND natural coagulant AND chemical coagulant AND efficiency; Treatment of wastewater AND natural coagulant AND chemical coagulant AND Moringa Oleifera). By applying this method, an extensive search was conducted in the title, abstract, and keywords of scholarly papers.

However, there are few articles included in the final analysis after considering few appropriate criteria. The selected criteria using inclusion and exclusion are listed in Table 1.

Table 1: List of criteria using inclusion and exclusion

Criteria	Decision
10 years of publications	Inclusion
The paper should be written in English	Inclusion
Article types are review and research articles	Inclusion
Papers that are duplicated within the search documents	Exclusion
Papers published before 2010	Exclusion
Papers that are not accessible	Exclusion

Figure 2 shows the flow diagram of screening the databases after going through a few screening processes which were screening through keywords, title and terms. In the next stage, the articles screening through the inclusion and exclusion criteria and the number of articles was reduced from 8751 to 1458. After the final screening by excluded the irrelevant articles through abstract screening, the number of articles was reduced from 1458 to 102.

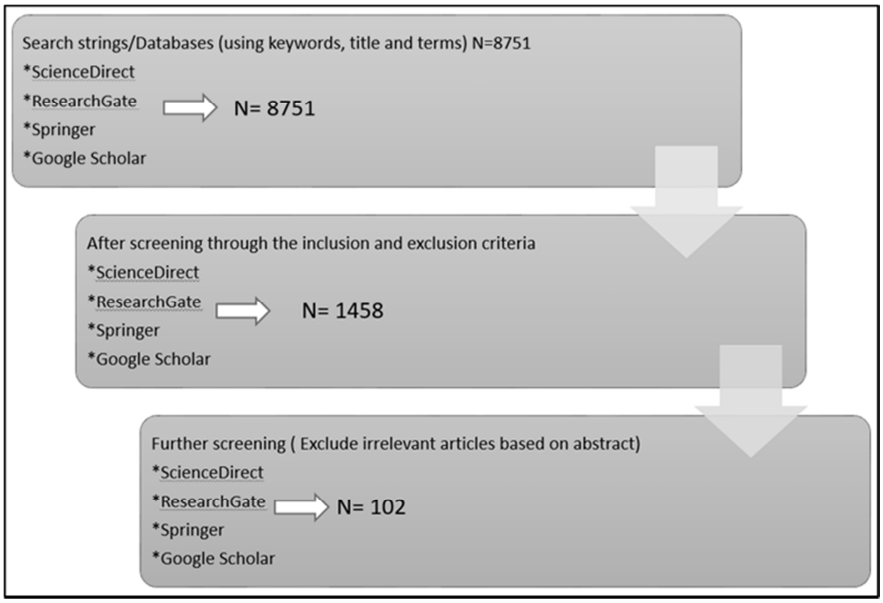

Figure 2: Flow diagram of screening the databases

3. MECHANISM OF COAGULANT

Impurities in wastewater appear as colloidal solid which is in the state of not readily settling down [8]. The existence of unsettled colloids produces the turbidity and color of wastewater. The colloid cannot be removed using a physical treatment process such as sedimentation. In general, the colloid and coagulant carry a negative charge and positively charged particles respectively. The negatively charged colloid will be attracted to positively charged coagulants and neutralized due to the electrostatic surface potential of the particles. In the end, floc will form due to the destabilization mechanism. Flocculation is a process of enhancing the floc to agglomerate forming bigger size particles so that it will settle down due to gravitational force. The mechanism of flocculation is polymer adsorption, polymer bridging and charge neutralization [9]. The polymer adsorption occurs if there is some affinity between the particle surface (pollutant) and polymer segments. Generally, the particle consists of plenty of attachment points for the polymer which means it is not necessary for the affinity between the particle and the polymer to be great. Polymer bridging is a process of linking the particles together with a long chain of polymer that consists of loops and tails.

3.1 Chemical coagulant

Two types of chemical coagulants are widely used in the wastewater treatment process which is an aluminium and iron metal-based coagulant. Aluminium sulphate or Alum is commonly used as a coagulant because of its effectiveness for turbidity removal in wastewater. As shown in Table 2, Alum shows great potential in removing turbidity of kaolin suspension with an initial concentration of 160 NTU by showing a quite high percentage of removal which is 99% [10]. Apart from that, in other research, they are using the application of combining chemical coagulant and natural coagulant for the water treatment process. They are combining Aluminium sulphate (Alum) and water-soluble Moringa Oleifera lectin to treat water in Recife, Pernambuco, Brazil with the turbidity removal of 91.3% [11]. Ferric Sulphate is also can be applied in wastewater treatment. It can achieve 98% of turbidity removal in kaolin suspension as shown in table 2. Besides, it has a special feature that is able to perform up to 86% removal of E.coli [10]. Aluminium chloride is very efficient to treat high turbidity wastewater. Based on previous research, aluminium chloride is able to treat 10000 NTU mixture of bentonite and deionized water by removing the turbidity by 99.5% [12]. On the other point of view, the application of aluminium chloride will produce more sludge because they are producing metal hydroxide [12]. Poly Aluminium chloride is widely used for water treatment in China. A study shows that it is effective to treat low turbidity of wastewater which is less than 10 NTU [13].

Table 2: Efficiency of chemical coagulants

Coagulant	Wastewater	Turbidity removal (%)
Aluminium sulphate (Alum), $Al_2(SO_4)_3$	Kaolin suspension	99
Ferric Sulphate, $Fe_2(SO_4)_3$	Kaolin suspension	98
Aluminium Chloride, $AlCl_3$	Clay	99.5

3.2 Natural coagulant

The natural coagulant is embedded with natural properties that made it an eco-friendly substance and harmless to human health. This will lead to a big opportunity for natural coagulants to replace chemical coagulants in the water treatment process as it may contribute to global sustainability. Based on the previous study, there are many types of natural coagulants that have great potential as a chemical coagulant in water treatment industries as shown in Table 3. Most plant-based coagulants have the potential to reduce the turbidity of water up to 99.7%. Besides that, it also shows the ability to reduce other factors such as suspended solids, Chemical Oxygen Demand (COD), sulphate and heavy metal content in the wastewater.

Table 3: Efficiency of natural coagulant

Effluent (Wastewater)	Coagulant	Optimal condition	Removal efficiency	Ref.
Concentrated latex effluent (7,243 NTU)	Dragon fruit foliage	pH 10 Dose: 500 mg/L	Turbidity removal: 99.7% COD: 94.7% Suspended solid (SS): 88.9%	[5]
Waste treatment plant intake (40.57 NTU)	Banana peel	pH 2 Dose: 110mg/L	Turbidity removal: 95%	[8]
Synthetic sewage	Banana peel	pH 1 Dose: 100mg/L	Turbidity removal: 88 %	[14]
Waste treatment plant intake (40.57 NTU)	Orange peel	pH 2 Dose: 110mg/L	Turbidity removal: 87.5%	[8]
Laundry rinsing water (83 NTU)	Orange peel	pH 8.2 Dose:6 ml/L	Turbidity removal: 89.5% TSS: 81.5%	[15]
Synthetic wastewater (200 NTU)	Moringa Oliefera	Dose:10 mg/L	Turbidity removal: 91.32%	[8]
Kaolin suspension (20 NTU-60 NTU)	Papaya seed	pH 6 Dose:0.2 mg/L -0.6 mg/L	Turbidity removal: 97.1%	[16]
Raw water (50 NTU-100NTU)	Jackfruit seed	pH 8 Dose: 40mg/L	Turbidity removal: 95.8%	[17]
Raw water (279 NTU)	Banana pith	pH 4 Dose: 0.1g/L	Turbidity removal: 98.56% COD: 54.37% SS: 96.03% Iron: 92.87% Copper: 100% Sulphate: 98.92%	[18]
Palm oil mill effluent (17,100 NTU-18,100 NTU)	Chickpea powder	pH 6.69 Dose: 2.6 g/L	Turbidity removal: 86% COD: 52%	[19]

			TSS: 87%	
Agro-industrial effluent TSS: 25,750 mg/L COD: 65,667 mg/L	Rice starch	pH 2.58 Dose: 0.74g/L	TSS: 92.50% COD: 31%	[20]
Palm oil mill effluent (26,670 NTU)	Chitosan	pH 4.51 Dose: 400 mg/L	Turbidity removal: 98.35% TSS: 98.95% COD: 68.31%	[21]
Dye solution (Congo Red) 200 mg/L	*Mucilaginous* seeds	pH 6.5 Dose: 1.6 mg/L	Dye removal: 68.5% COD: 61.6%	[22]
Dye solution (Congo Red) 250 mg/L	Maize	pH 4.0 Dose:	Colour removal: 89.4%	[23]

4. CHARACTERIZATION OF NATURAL COAGULANT

In general, natural coagulants consist of specific molecular compositions with effective functional groups such as carboxyl and hydroxyl groups to neutralize and link the colloidal particle together in the wastewater treatment process [24]. To achieve effective destabilisation, the natural coagulant should have a chemical group which is a free hydroxyl group with binding sites that can react with the sites on the surface of the colloidal particles [25]. J.K Fatombi et al reported that copra (Cocos nucifera) shows a peak around 3411 cm^{-1} to 3290 cm^{-1} based on the recorded value from FTIR which indicates that the existence of hydroxyl group [26].

Apart from that, there was research found that powdered chickpea recorded wavelength within the range of 3600 to 3100 cm^{-1} with the peak at 3276.11 cm^{-1} which indicates the presence of hydroxyl group [27]. Based on the finding, the Cicer Arietinum manage to achieve 86% of turbidity removal. Based on the FTIR analysis by Wennie Subramonian et al, Cassia obtusfolia seed gum has a broad and strong band at 3277 cm^{-1} due to O-H stretching and the presence of a C-H bond was indicated at 2923 cm^{-1}. Moreover, the Cassia obtusfolia seed manage to achieve 86.9% of total suspended solids removal and 36.2% of chemical oxygen demand removal [28].

Sze Yin Cheng et al had conducted research on landfill leachate treatment using guar gum powder as a natural coagulant. It was found that it has a strong and broad peak at 3308 cm^{-1} and another narrower peak at 1017.49 cm^{-1} that prove the presence of O-H and C-O stretch respectively. Moreover, it was observed that the presence of a carboxyl group at a peak of 1800 cm^{-1} could help in the coagulation process by forming ion bridges and site binding [29].

5. EFFECT OF MIXING CONDITIONS

The efficiency of the coagulant is based on an appropriate selection of coagulant and optimization of process parameters such as pH, a dosage of coagulant, mixing time, settling time etc. The treatment efficiency could be significantly increased as the appropriate optimization of the parameters were obtained.

The mixing condition is very important in the coagulation-flocculation of the wastewater treatment process. Good mixing conditions will ensure excellent floc properties. In general, there are two stages of mixing which are first fast mixing and subsequent slow mixing stage respectively. The purpose of the first fast mixing stage is to ensure the coagulant is uniformly distributed into the suspension whereas the subsequent slow mixing stage is to ensure the organic are adsorbed onto the natural coagulant before precipitation [30], [31]. Increasing mixing time lead to a decrease in the final floc size [32] and fast-settling particles can be achieved by maximizing the size of aggregation of the small particles [33]. Jian Zhe et al evaluated that the breakage and recovery factor decreases as the rapid stirring speed increases [34].]. The finding of mixing conditions were shown in Table 4.

Sze Yin Cheng has affirmed that the flocs formed using guar gum is strong and compact with a speed of 100 rpm as compared with rice starch with a mixing speed of 10 rpm [29]. The gum chain polymer has a vital role to ensure a strong formation of flocs which could help avoid breakage happened due to stretching mechanism that may happen before actual breakage due to the flexibility of the polymers [35]. Research of coagulation process of kaolin suspension using liquid bitter coagulant shows that large flocs were formed at 120 rpm of fast mixing speed as compared with 100 rpm [36]. Ezeh Ernest et al reported that watermelon seed shows the highest coagulant efficiency with the mixing speed of 120 rpm as compared with 40 rpm and 200 rpm [37].

Table 4: Mixing condition of several types of coagulant

Coagulant	Wastewater	Mixing condition	Ref
Guar gum	Leachate	Mixing speed: 100 rpm	[29]
Liquid bitter	Kaolin suspension	Mixing speed: 120 rpm	[36]
Watermelon seed	River water	Mixing speed: 120 rpm	[37]

6. EFFECT OF SETTLING TIME

Coagulant refers to a process of rapid mixing that disperses coagulant to form microflocs in wastewater while flocculation refers to a process of slow mixing to aggregate microflocs to form macroflocs which can be settled [38].

Meysam Mohammad Momeni et al investigated that settling time is an independent factor that impacts a significant effect on the turbidity removal efficiency [39]. It also shows that the turbidity removal increases as the settling time increases. Based on their finding, the optimum settling time is 78.93 minutes with 90.14% turbidity removal. Yasir Talib Hameed et al researched a tannin-based agent for coagulation and flocculation of municipal wastewater with settling time ranged from 2 minutes to 10 minutes. They found that the highest turbidity reduction was from 8 NTU to 5.2 NTU with 10 minutes of settling time [38].

In other research of chitosan, Henry K. Agbovi et al conducted a coagulation and flocculation process with settling time ranged from 0 minutes to 60 minutes. Based on their finding, there are no changes for the flocculation efficiency after 30 minutes which indicates that 30 minutes is the optimum settling time [39]. The data were tabulated in Table 5.

Table 5: The effect of settling time on the efficiency of various types of natural coagulants.

Coagulant	Wastewater	Settling time (mins)	Efficiency	Ref
Chitosan	Industrial wastewater (300 NTU)	(40-120) 78.93	Turbidity removal: 90.14% Colour removal: 76.20%	[39]
	Kaolin suspension (400 NTU)	(0-60) 30	Turbidity removal: 95.8%	[40]
Tannin	Municipal wastewater (68 NTU)	(2-10) 10	Turbidity removal: 91.03%	[38]
Polyamines	Raw water (34.46 NTU)	(10-40) 20	Turbidity removal: 72%	[41]
Alum-modified cassava peel starch	Raw water (26.06 NTU)	(10-120) 10	Total suspended solid (TSS) removal: 92.75%	[42]
Polysilicate magnesium	Dye wastewater (300 NTU)	(5-40) 20	Colour removal: 94%	[43]

7. CONCLUSION

In conclusion, the plant-based coagulant is an excellent coagulant for a variety of types of the wastewater treatment process. Based on the finding, all natural coagulant shows high turbidity removal which is approximately above 80%. The high turbidity removal shows that natural coagulant is the other alternative to replace chemical coagulants which have the downside for human health and the environment. Apart from that, these natural coagulants can reduce chemical oxygen demand (COD), total suspended solids (TSS) and heavy metal content in the wastewater. Based on the FTIR analysis, the presence of functional groups such as carboxyl and hydroxyl help to improve the coagulation and flocculation in the wastewater treatment process. There are few factors that will be influencing the efficiency of coagulants in the wastewater treatment process. The efficiency of the coagulant is based on an appropriate selection of coagulant and optimization of process parameters such as pH, a dosage of coagulant, mixing time, settling time etc. The optimum condition will enhance the maximum potential of the coagulant. Besides that, it helps to control the usage of coagulant which is good in terms of economic perspective. The mixing condition is one of the important factors in the wastewater treatment process. Good mixing conditions will ensure excellent flocs properties. The efficiency of the coagulant can be evaluated based on the flocs condition during the process. Based on the finding, the best mixing speed for the jar test is around 100-120 rpm.

ACKNOWLEDGEMENTS

The authors would like to express gratitude for the support given by the Universiti Teknologi MARA Cawangan Pulau Pinang.

8. REFERENCES

1. Y.Shan, D.Guan, J.Liu, Z.Liu, L.Jingru, H.Schroeder, Y.Chen, S.Shao, Z.Mi, and Q.Zhang**,** CO_2 emissions inventory of Chinese cities, Atmos. Chem. Phys. Discuss.(2016) 1–26.
2. T. Popovic, A. Kraslawski, and Y. Avramenko, Applicability of sustainability indicators to wastewater treatment processes, Elsevier B.V, 32. 2013.
3. F. Renault, B. Sancey, P. M. Badot, and G. Crini, Chitosan for coagulation/flocculation processes - An eco-friendly approach, Eur. Polym. J. 45 (2009) 1337–1348.
4. N. A. Oladoja, Headway on natural polymeric coagulants in water and wastewater treatment operations, J. Water Process Eng. 6 (2015) 174–192.
5. J. Idris, A. M. Som, M. Musa, K. H. Ku Hamid, R. Husen, and M. N. Muhd Rodhi, Dragon fruit foliage plant-based coagulant for treatment of concentrated latex effluent: Comparison of treatment with ferric sulfate, J. Chem., (2013)1-7.
6. V. Kumar, N. Othman, and S. Asharuddin, Applications of Natural Coagulants to Treat Wastewater - A Review, MATEC Web Conf. 103 (2017)1–9.
7. W. Mengist, T. Soromessa, and G. Legese, Method for conducting systematic literature review and meta-analysis for environmental science research, MethodsX, 7 (2020) 100777.
8. N. S. Zaidi, K. Muda, L. W. Loan, M. S. Sgawi, M. Adibah, and A. Rahman, Potential of Fruit Peels in Becoming Natural Coagulant for Water Treatment, 1(2019) 140–150.
9. B. Bolto and J. Gregory, Organic polyelectrolytes in water treatment. 41(2007) 2301–2324.
10. M. Pritchard, T. Craven, T. Mkandawire, A. S. Edmondson, and J. G. O'Neill, A comparison between Moringa oleifera and chemical coagulants in the purification of drinking water - An alternative sustainable solution for developing countries, Phys. Chem. Earth, 35 (2010) 798–805.
11. J.H.E.S. Freitas, K.V. Santana, A.C.Claudinado Nascimento, S. Carvalhode Paiva, M.C. Moura, L.C.B. BarrosoCoelho, M.B.M.Oliveira, P.M. Paiva, A.E. Nascimento, T.HenriqueNapoleão, Evaluation of using aluminum sulfate and water-soluble Moringa oleifera seed lectin to reduce turbidity and toxicity of polluted stream water, Chemosphere. 163(2016) 133–141.
12. C. Y. Hu, S. L. Lo, C. L. Chang, F. L. Chen, Y. De Wu, and J. L. Ma, Treatment of highly turbid water using chitosan and aluminum salts, Sep. Purif. Technol. 104 (2013) 322–326.
13. R. Jia, Y. Bai, and J. Yang, Experimental research on the poly-aluminum chloride for treating the Pi River water in winter and summer, IOP Conf. Ser. Earth Environ. Sci. 113 (2018)1–7.
14. M. Priyatharishini, N. M. Mokhtar, and R. A. Kristanti, Study on the Effectiveness of Banana Peel Coagulant in Turbidity Reduction of Synthetic Wastewater, Int. J. Eng. Technol. Sci., vol. ISSN, no. 1 (2019) 2462–1269.
15. S. M. Mohan, Use of naturalized coagulants in removing laundry waste surfactant using various unit processes in lab-scale, J. Environ. Manage.136 (2014)103–111.
16. J. R. Jeon, E. J. Kim, Y. M. Kim, K. Murugesan, J. H. Kim, and Y. S. Chang, Use of grape seed and its natural polyphenol extracts as a natural organic coagulant for removal of cationic dyes, Chemosphere, vol. 77. 8(2010)1090–1098.
17. R. Natumanya and J. Okot-Okumu, Evaluating coagulant activity of locally available Syzygium cumini, Artocarpus heterophyllus and Moringa oleifera for treatment of community drinking water, Uganda, Int. J. Biol. Chem. Sci.9(2016) 2535.
18. B. Kakoi, J. W. Kaluli, P. Ndiba, and G. Thiong'o, Banana pith as a natural coagulant for polluted river water, Ecol. Eng. 95(2016) 699–705.
19. B. L. Choong Lek et al., Treatment of palm oil mill effluent (POME) using chickpea (Cicer arietinum) as a natural coagulant and flocculant: Evaluation, process optimization and characterization of chickpea powder, J. Environ. Chem. Eng.6 (2018) 6243–6255.

20. C. Y. Teh, T. Y. Wu, and J. C. Juan, Optimization of agro-industrial wastewater treatment using unmodified rice starch as a natural coagulant, Ind. Crops Prod.56 (2014) 17–26.
21. A. H. Jagaba et al., Sustainable use of natural and chemical coagulants for contaminants removal from palm oil mill effluent: A comparative analysis, Ain Shams Eng. J., Mar. 2020.
22. S. Shamsnejati, N. Chaibakhsh, A. R. Pendashteh, and S. Hayeripour, Mucilaginous seed of Ocimum basilicum as a natural coagulant for textile wastewater treatment, Ind. Crops Prod. 69(2015) 40–47.
23. H. Patel and R. T. Vashi, Removal of Congo Red dye from its aqueous solution using natural coagulants, J. Saudi Chem. Soc., vol. 16 (2012)131–136.
24. B. C. Lim, J. W. Lim, and Y. C. Ho, Garden cress mucilage as a potential emerging biopolymer for improving turbidity removal in water treatment, Process Saf. Environ. Prot., vol. 119 (2018) 233–24.
25. C. S. Lee, M. F. Chong, J. Robinson, and E. Binner, A review on development and application of plant-based bioflocculants and grafted bioflocculants, Industrial and Engineering Chemistry Research. 48(2014)18357–18369.
26. J. K. Fatombi, B. Lartiges, T. Aminou, O. Barres, and C. Caillet, A natural coagulant protein from copra (Cocos nucifera): Isolation, characterization, and potential for water purification, Sep. Purif. Technol.116(2013) 35–40.
27. B. L. Choong Lek et al., Treatment of palm oil mill effluent (POME) using chickpea (Cicer arietinum) as a natural coagulant and flocculant: Evaluation, process optimization and characterization of chickpea powder, J. Environ. Chem. Eng. 6 (2018) 6243–6255.
28. W. Subramonian, T. Y. Wu, and S. P. Chai, A comprehensive study on coagulant performance and floc characterization of natural Cassia obtusifolia seed gum in treatment of raw pulp and paper mill effluent, Ind. Crops Prod. 61(2014) 317–324.
29. S. Y. Cheng et al., Sustainable landfill leachate treatment: Optimize use of guar gum as natural coagulant and floc characterization, Environ. Res. 188 (2020)109737.
30. A. Kumar Giri, J. Kumar, and G. Warnecke, The continuous coagulation equation with multiple fragmentation, J. Math. Anal. Appl. 374(2011)71–87.
31. M. A. Yukselen and J. Gregory, Breakage and Re-formation of Alum Flocs, Environ. Eng. Sci. 19(2002) 229–236.
32. W. zheng Yu, J. Gregory, L. Campos, and G. Li, The role of mixing conditions on floc growth, breakage and re-growth, Chem. Eng. J.2 (2011) 425–430.
33. T. Serra, J. Colomer, and B. E. Logan, Efficiency of different shear devices on flocculation. Water Res.42 (2008) 1113–1121.
34. J. Zhao, R. Su, X. Guo, W. Li, and N. Feng, Role of mixing conditions on coagulation performance and flocs breakage formed by magnesium hydroxide, J. Taiwan Inst. Chem. Eng., 45 (2014) 1685–1690.
35. J. Gregory and S. Barany, Adsorption and flocculation by polymers and polymer mixtures, Advances in Colloid and Interface Science, vol. 169, no. 1. Elsevier B.V. (2011)1–12.
36. S. BinAhmed, G. Ayoub, M. Al-Hindi, and F. Azizi, The effect of fast mixing conditions on the coagulation–flocculation process of highly turbid suspensions using liquid bittern coagulant, Desalin. Water Treat. 53 (2015) 3388–3396.
37. E. Ernest, O. Onyeka, N. David, and O. Blessing, Effects of pH, Dosage, Temperature and Mixing Speed on The Efficiency of Water Melon Seed in Removing the Turbidity and Colour of Atabong River, Awka-Ibom State, Nigeria, Int. J. Adv. Eng. 3(2017) 427-343.
38. Y. T. Hameed, A. Idris, S. A. Hussain, N. Abdullah, H. C. Man, and F. Suja, A tannin–based agent for coagulation and flocculation of municipal wastewater as a pretreatment for biofilm process, J. Clean. Prod. 182 (2018) 198–205.

39. M. M. Momeni, D. Kahforoushan, F. Abbasi, and S. Ghanbarian, Using Chitosan/CHPATC as coagulant to remove color and turbidity of industrial wastewater: Optimization through RSM design, J. Environ. Manage.211 (2018) 347–355.
40. H. K. Agbovi and L. D. Wilson, Design of amphoteric chitosan flocculants for phosphate and turbidity removal in wastewater, Carbohydr. Polym.189 (2018) 360–370.
41. A. Cainglet, A. Tesfamariam, and E. Heiderscheidt, Organic polyelectrolytes as the sole precipitation agent in municipal wastewater treatment, J. Environ. Manage. 271(2020) 111002.
42. S. M. Asharuddin, N. Othman, N. S. M. Zin, H. A. Tajarudin, and M. F. Md Din, Flocculation and antibacterial performance of dual coagulant system of modified cassava peel starch and alum, J. Water Process Eng. 31 (2019) 100888.
43. Y. Wei, Q. Ji, L. Chen, J. Hao, C. Yao, and X. Dong, Preparation of an inorganic coagulant-polysilicate–magnesium for dyeing wastewater treatment: Effect of acid medium on the characterization and coagulation performance, J. Taiwan Inst. Chem. Eng.72 (2017)142–148. 2017.

THE EFFECT OF HIDDEN LAYER, NEURON NUMBERS AND THE ACTIVATION FUNCTION ON THE ARTIFICIAL NEURAL NETWORK ACCURACY ON FIBER REINFORCED CONCRETE SHEAR RESISTANCE PREDICTION

Syahrul Fithry Senin[1*], Amer Yusuf[2] and Rohamezan Rohim[3]
[1, 2] *College of Engineering, School of Civil Engineering, UiTM Cawangan Pulau Pinang, Kampus Permatang Pauh, MALAYSIA.*
(E-mail: syahrul573@uitm.edu.my, ameryusuff@uitm.edu.my)
[3] *College of Engineering, School of Civil Engineering, UiTM Cawangan Pulau Pinang, Kampus Permatang Pauh, MALAYSIA..*
(E-mail: rohamezan627@uitm.edu.my)

ABSTRACT- Artificial Neural Network is widely used in the prediction of the shear resistance of fibre reinforced concrete beam. The process of optimizing this network for obtaining simple, yet global minimum error is of civil engineers interest. The work is focussed on a trial and error approach, on obtaining the optimal network for shear resistance prediction of fibre reinforced concrete beams, by selecting appropriate combination of hidden layer, its neuron numbers and fourteen types of activation function. By using logsig as the activation function and by employing 6 neuron numbers in the network, the Root Mean Square Error value will be the lowest, which yield the most optimal neural network. This optimal network, will be then validated with the testing and validation datasets to observe its prediction accuracy on the shear resistance.

Keywords: Artificial Neural Network, Activation function, Hidden Layer, Neuron Number, Root Mean Square Error, SFRC.

1. INTRODUCTION

When a plain concrete beam is exposed to certain tensile stresses this beam will crack due to the excessive shear stresses [1]. This shear crack failure will appear suddenly and without warning, especially in reinforced concrete beams; usually causes catastrophic damage to both humans and property. The usage of these steel fibers in concrete will also increase the overall shear resistance of steel fiber-reinforced concrete (SFRC) beams by improving the tensile stress threshold value at the post-cracking level [2]. Because the mechanisms underlying this shear resistance are unclear, it is critical to explore the contributing elements such as the volume of SFRC, the dimension of beam geometry, the aggregate silica content, and the compression strength. Several model expressions [3-6] and current algorithms [7] have been produced via expensive laboratory testing of full-scale beams, and these expressions are frequently semi-empirical, with significant limitations in their accuracies. Because there are no simple equations or charts that explain shear resistance for fiber reinforced concrete (SFRC) beams, there is a need to develop a feasible computational solution that can be utilized to predict shear resistance in SFRC.

Artificial Neural Network (ANN) is a potential Machine Learning technology that can be utilized in a variety of civil engineering applications to model complex input-output parameters. An ANN is made up of multiple fundamental components that are stacked in layers, such as neurons. A neuron has a single output and numerous inputs. The input layer collects incoming input and sends it to the hidden layer, where it is interpreted by adding it all together and applying it to the activation function as an output function. Back Propagation Neural Networks (BPNNs) are the most frequent technique used by civil engineer researchers to train research datasets [8].

The determination of the number of hidden layer numbers and its neurons numbers is one of the issues confronted by researchers in ANN modelling [9]. This is crucial since it will have a significant impact on the predicted results. As a result, a careful balance between the hidden layers and the neuron numbers in each layer must be determined, as well as the activation function. To reduce the computational time, ANN modelling and prediction of SRFC shear resistance will be undertaken in this article using only one hidden layer. The performance of a single hidden layer network trained with the Leverberg-Marquard technique is monitored by MATLAB software in this research. On constructing the best ANN model, the parameters related to ANN training as well as the design parameters are considered. A case study on a small dataset of 42 shear resistance datasets is shown to showcase the experimental details and its results.

2. EXPERIMENTAL DETAILS

Forty-two (42) SFRC datasets extracted from ten independent physical experimental research works (Amin & Foster[10] ; Amin et al.[11] ; Greenough & Nehdi[12] ; Hwang et al. [13]; Imam et al., [14]; Kwak et al., [15]; Qissab & Salman,[16]; B. Singh & Jain, [17]; Spinella, [18]; Zarrinpour & Chao [19]) were used in this preliminary study. Table 1 shows the statistics of the datasets, with all of them having a shear span to depth ratio more than 2.5, indicating that shear dominates the failure process.

Table 1. Ranges of Parameters in Database

Parameter (units)	Min	Max
bw (mm)	100	150
h (mm)	150	300
d (mm)	135	251
fck (MPa)	24.9	68.6
Vf (%)	0.5	1.0
da (mm)	5	20
Vutot (kN)	900	2400

where bw, h, d, fck, Vf, da and Vutot is the web width, width of beam, depth of beam, concrete compression strength, volume of fiber, size of the aggregate and the ultimate shear resistance, respectively,

The log-normal transformation is used to transform these datasets to approximate normalcy [20], ensuring that the total data has a roughly symmetric bell-shaped distribution. Only one hidden layer was used in this investigation to reduce modelling computation time. The performance metric of the ANN was explored by altering the neurons counts from 1 to 10 and using 14 types of activation functions (Table 2) to discover the most optimum number of hidden neurons in one hidden layer. The ANN's performance metric is the Root of Mean Square Error (RMSE), which is defined as follows.

$$RMSE = \sqrt{\sum_{i=1}^{N} \frac{\left(Y_p^i - Y_a^i\right)^2}{N}}$$

where Y_p^i, Y_a^i, N is the predicted shear resistance, the actual shear resistance from datasets and the number of datasets used (42 numbers) in the computation respectively.

The datasets were separated into subsets for training, validation, and testing to establish a viable model. The remaining datasets will be divided evenly for network dependability and to minimize overfitting, with 70 percent of the datasets being evaluated for network training. During the training cycle, the trained ANN model's convergence is based on minimizing the root of mean square error (RMSE) value. The total performance of the trained network is measured by comparing the predicted shear resistance to actual output from the datasets listed in Table 1.

Table 2. List of Activation Functions Used

Number	Activation Function
1	compet
2	elliotsig
3	hardlim
4	logsig
5	hardlims
6	netinv
7	poslin
8	purelin
9	radbas
10	radbasn
11	satlin
12	satlins
13	softmax
14	tansig

3. RESULTS AND DISCUSSION

The effect of the neuron number and the activation function on the ANN performance training metric

Figure 1(a)-(c) shows the ANN performance metric on training 42 datasets by varying the neuron number from 1 to 10. The first five activation functions (compet, elliotsig, hardlim, hardlims and logsig), the second five activation functions (netinv, poslin, radbas, radbasn) and the final four activation functions (satlin, satlins, softmax, tansig) were used during the training of ANN modelling on shear resistance prediction of SFRC.

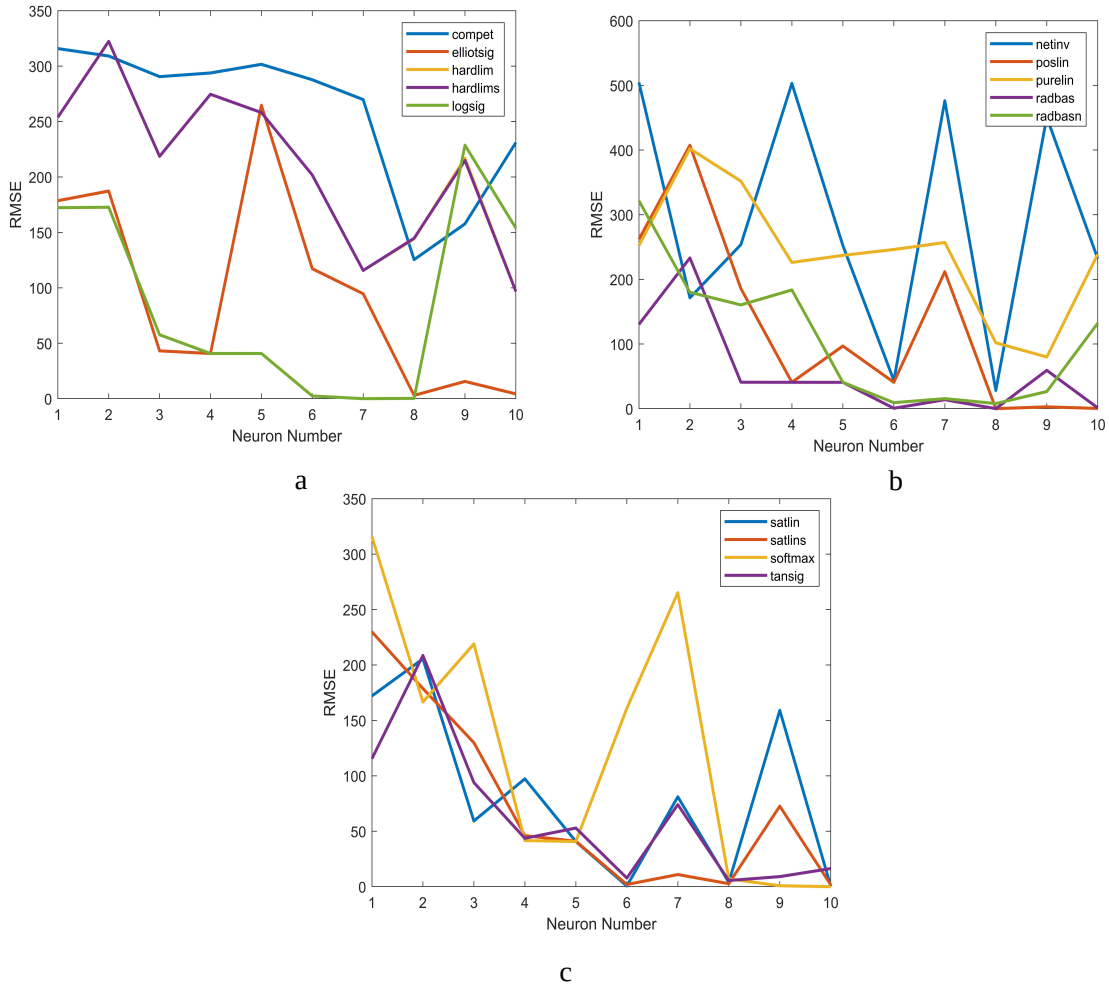

Figure 1. ANN performance metric for (a) first five activation functions(b) second five activation functions, and (c) the final four activation functions

It can be observed that, generally, RMSE values were decreases as the neuron number increases when the datasets were train under different activation functions. However, by using logsig, radbasn and satlins, the ANN metric performance was showed to be more stable as the RMSE values always decreased consistently when neuron number is increasing from 1 to 7 as shown in Figure 2. It can be inferred that the optimum number of neuron number for datasets training is 6 as the RMSE values increases for all activation function shown in Figure 2, and 'logsig' is the activation function that produce lowest RMSE values for the shear resistance prediction.

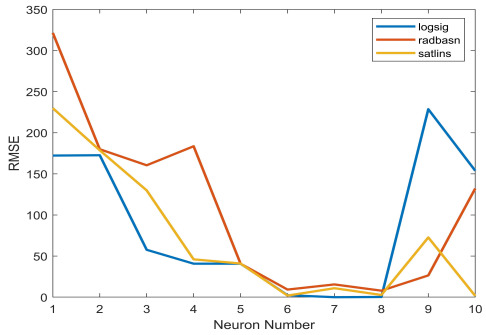

Figure 2. ANN performance metric for three activation functions

4. CONCLUSION

In this study, various activation functions with varying number of neuron numbers have been used to access the performance of shear resistance predictions. It was found that by using logsig as the activation function and 6 number of neurons, the network able to predict the shear resistance of SFRC beam accurately.

Future works will be focused on studying the behavior of the validation and testing network performance under the same number of neuron and activation function.

ACKNOWLEDGEMENTS

The authors would like to express gratitude for the support given by the Universiti Teknologi Mara Cawangan Pulau Pinang, Kampus Permatang Pauh.

5. REFERENCES

1. L. Xuesen, D. Jie, D. Mingke. Shear Behavior of High Ductile Fiber Reinforced Concrete Beams, Alexandria Engineering Journal, Vol.60, No.1, 1665-1675.
2. S. Mansor, R.N. Mohamed, N.A. Shukri, M.S.N. Mahmoor, N. Azilah, F. Zamri. Overview on the Theoretical Prediction of Shear Resistance of Steel Fibre in Reinforced Concrete Beam, IOP Conference Series: Earth and Environmental Science, doi:10.1088/1755-1315/220/1/012033, 1-10, 2019.
3. J.H. Hwang, D.H. Lee, H. Ju, H. Kim, K.S. Seo, S.Y. Kang, J.W. Kang. Shear behavior models of steel fiber reinforced concrete beams modifying softened truss model approaches, Materials, Vol. 6, No. 10, 4847-4867.
4. J.A.O. Barros, S.J. Foster. An Integrated Approach for Predicting the Shear Capacity of Fibre Reinforced Concrete Beams, Engineering Structures, Vol. 174, 346-357.
5. Y.C. Choi, J.H. Moon, E.J. Lee, K.S. Park, K.S. Lee. Development of Shear Strength Equation for Beam-Column Connections in Reinforced Concrete and Steel Composite System, International Journal of Concrete Structures and Materials, Vol. 11, No. 2, 185-197.
6. N. Spinella. Shear Strength of a Full-Scale Steel Fibre-Reinforced Concrete Beams without Stirrups, Computers and Structures, Vol. 11, No. 5, 365-382.

7. A. Luigi, National Research Council, Guide for the Design and Construction of Fiber-Reinforced Concrete Structures, Advisory Committee on Technical Recommendations for Construction, CNR-DT 204/2006, 1-55.
8. A.Hojjat. Neural Network in Civil Engineering: 1989-2000, Computer-Aided Civil and Infrastructure Engineering, Vol. 16, No. 2, 126-142.
9. K.G. Sheela, S.N. Deepa. Review on Methods to Fix Number of Hidden Neuron in Neural Networks, Mathematical Problems in Engineering, Vol. 2013, https://doi.org/10.1155/2013/425740.
10. S. Kiran, B. Lal. Modelling of Soil Shear Strength Using Neural Network Approach, EJGE, Vol. 21, No. 2016, 3751-3771.
11. A. Amin, S.J. Foster. Shear Strength of Steel Fibre Reinforced Concrete Beams with Stirrups, Engineering Structures, Vol. 111, 323-332.
12. A. Amin, S.J. Foster, M. Watts. Modelling the tension stiffening effect in SFR-RC, Magazine of Concrete Research, Vol. 68, No. 7, 339-352.
13. T. Greenough, M.L. Nehdi. Shear Behavior of Fiber-Reinforced Self-Consolidating Concrete Slender Beams, Materials Journal, Vol. 105, No. 5, 468-477.
14. M. Imam, L. Vandewalle, F. Mortelmans, D.V. Gemert. Shear domain of fibre-reinforced high-strength concrete beams, Engineering Structures, Vol. 19, No. 9, 738-747.
15. Y. Kwak, M.O. Eberhard, W. Kim, J. Kim. Shear Strength of Steel Fiber-Reinforced Concrete Beams without Stirrups, Structural Journal, Vol. 99, No. 4, 530-538.
16. M.A. Qissab, M.M. Salman. Shear strength of non-prismatic steel fiber reinforced concrete beams without stirrups, Structural Engineering and Mechanics, Vol. 67, No. 4, 347-358.
17. B, Singh, K. Jain. Appraisal of steel fibers as minimum shear reinforcement in concrete beams, ACI Structural Journal, Vol. 111, No. 5, 1191-1202.
18. M. Spinella. Shear strength of full-scale steel fibre-reinforced concrete beams without stirrups, Computers and Concrete, Vol. 11, No. 5, 365-382.
19. M.R. Zarrinpour, S.H. Chao. Shear strength enhancement mechanisms of steel fiber-reinforced concrete slender beams, ACI Structural Journal, Vol. 114, No. 3, 729-742.
20. C. Feng, H. Wang, N. Lu, T. Chen, H. He, Y. Lu, X.M. Tu. Log Transformation and its Implications for Data Analysis, Shanghai Archives of Psychiatry, Vol. 26, No. 2, 105-109.

REMOTE SENSING STUDY OF THE RAINFALL INTENSITY OVER PENANG ISLAND IN TIME SERIES

Mohamad Mubarak Mohamad Yakzan[1], Mohd Muzafa Jumıdalı[2], Fathınul Najıb Ahmad Sa'ad[3], Abd Rahman Mat Amin[4]*

[1]Faculty of Chemical Engineering, Universiti Teknologi MARA, 13500, Permatang Pauh, Penang, Malaysia
[2]Faculty of Applied Science, University Teknologi MARA, 13500, Permatang Pauh, Penang Malaysia.
[3]Faculty of Applied Science, University Teknologi MARA, 40450 Shah Alam, Selangor Malaysia
[4]Faculty of Applied Science, Universiti Teknologi MARA, 23200 Bukit Besi, Terengganu, Malaysia
**mohdmuza433@uitm.edu.my*

ABSTRACT- The study explored the remote sensing of rainfall intensity over Penang Island in time series. Penang Island is being selected as a study area because it is suitable in term of variation in weather condition that affects the intensity of rainfall. The intensity of rainfall can be monitored by using the GIOVANNI system. GIOVANNI system is utilized to get information from satellites to empower Web-based visualization and investigation of satellite remotely without users having to download data. By using the GIOVANNI system, the prediction of future events can be plotted through the time series of rainfall where TOVAS is used as a sensor to measure the intensity of rainfall. The time series of rainfall can be plotted daily, monthly or yearly depending on the purpose of study. The main purpose of this study is to verify the reliability of the NASA GIOVANNI yearly data by comparing with real data from WORLD WEATHER. The both data is compared by doing cross validation using regression analysis where R-square as an indicator to determine whether the relationship between both data is strong or weak. The results from this study show that the R-square for the data for 2016 and 2017 are 0.4295 and 0.4743 respectively. R-square value is lower than 0.5 where it is considered a weak relationship between data from the GIOVANNI system and WOLRD WEATHER data.

Keywords: *GIOVANNI system, WORLD WEATHER, regression analysis, time series, TOVAS*

1. INTRODUCTION

Rainfall intensity is defined as the ratio of the total amount of rain falling over time and is expressed in units of depth per unit time, usually as mm per hour (mm/h) [1]. The concentration of precipitation can be measured within the height of the water layer that covers the ground over a period of time [2]. It means that the rain that stays where it falls will form a layer of rainwater at a certain height. The intensity of rainfall can be high or low because it depends on the local circumstances. In general, a low intensity is, for instance, 2 mm of rainwater a day and then a high of around 30mm an hour. high intensity of rainfall can lead to flash floods because soil is unable to absorb the water in the area it falls [3]. As a result, that water remains on the top of the ground. There are three main types of rainfall, which are relief rainfall, frontal rainfall and convection rainfall where Penang Island has these type of rain [4].

Penang Island gets a tropical climate throughout the year. This means it is warm and humid throughout the year with variations in weather conditions. There are many bad effects if the intensity of rainfall is too high or too low, such as flooding, landslides, or insufficient water. Penang Island is one of the states in Malaysia that is always hit by flash floods. The floods that have happened are not about drainage issues, but about the intensity of rainfall [5] in that area. The driest weather in Penang is in January when an average of 68.7 mm and the wettest weather is in October when an average of 383 mm of rainfall occurs [3]. Besides that, rainfall can also affect economic activities in Penang if it is of high intensity. For example, Penang International Airport (PIA) experienced flight delays for around half an hour due to high rainfall intensity [5]. In fact, the high intensity of rainfall on the West Coast, which is Penang, is because of the inter-monsoon period of April-May and September-October [6]. Regarding of that factors, it's very important to access the data of rainfall to make prediction of future events.

In order to access the data on rainfall easily, remote sensing which GIOVANNI interface for climatic information is utilized. GIOVANNI is one of the pioneering Web services provided to the public for the analysis of NASA Earth science data. GIOVANNI has given users, both neophytes and experts, a way to explore remote sensing and model data with minimal investment in time and software. As it has grown and evolved, GIOVANNI has added many more analytical capabilities, and has markedly improved system performance and speed. GIOVANNI is used to empower Web-based visualization and investigation of satellite remotely detected meteorological, oceanographic, and hydrologic information sets without users having to download data [7]. The current GIOVANNI operating system framework contains eight distinctive interfaces, which allow the preparation of several important satellite measurements. Depending on the input information structure, the framework gives diverse straightforward measurable investigation and makes numerous valuable plot sort pictures or ASCII yields [8]. In this study, by using GIOVANNI system, the data of rainfall can be access where TOVAS is used as a sensor to measure the intensity of rainfall in this system. TOVAS can provide data at three different levels, which are level one, level two and level three. Level one can be characterized as unprocessed instrument data at full resolution, time reference, and annotated with ancillary information. Then, radiometrically corrected geolocated for the next process. For the level two data, it derived geophysical parameters at the same resolution and location as those of the Level 1 data [9]. TOVAS is very suitable sensor where it's commonly used for rainfall algorithm study.

The main purposes of the study are to verify the reliability of satellite data using the GIOVANNI system with real data, both of which will be compared in order to determine the relationship between them by doing cross validation using regression analysis [10]. Then, R-square from regression analysis is used as an indicator in order to determine whether the relationship between both data sets is strong or weak.

2. EXPERIMENTAL DETAILS

2.1 GIOVANNI System

The GIOVANNI system was the chosen strategy in this research. It was created to permit users to deliver intelligent examinations online without downloading any data. The GIOVANNI system

makes gridded data accessible in a specific arrangement that anybody can learn to utilize in minutes and put to work beneficially for research or applications. The GIOVANNI framework has been examined as a valuable method for accessing numerous distinctive sorts of remote detection data. Through the GIOVANNI, an assortment of environmental information types have been permitted for diverse application regions such as agribusiness, hydrology, and air quality research. The GIOVANNI system can be a direct Web application. The main Web page contains a title, a brief depiction of the area, and an expressive list of one or more GIOVANNI arrangements accessible. Figure 1 and Figure 2 show the main Web page and GIOVANNI application system.

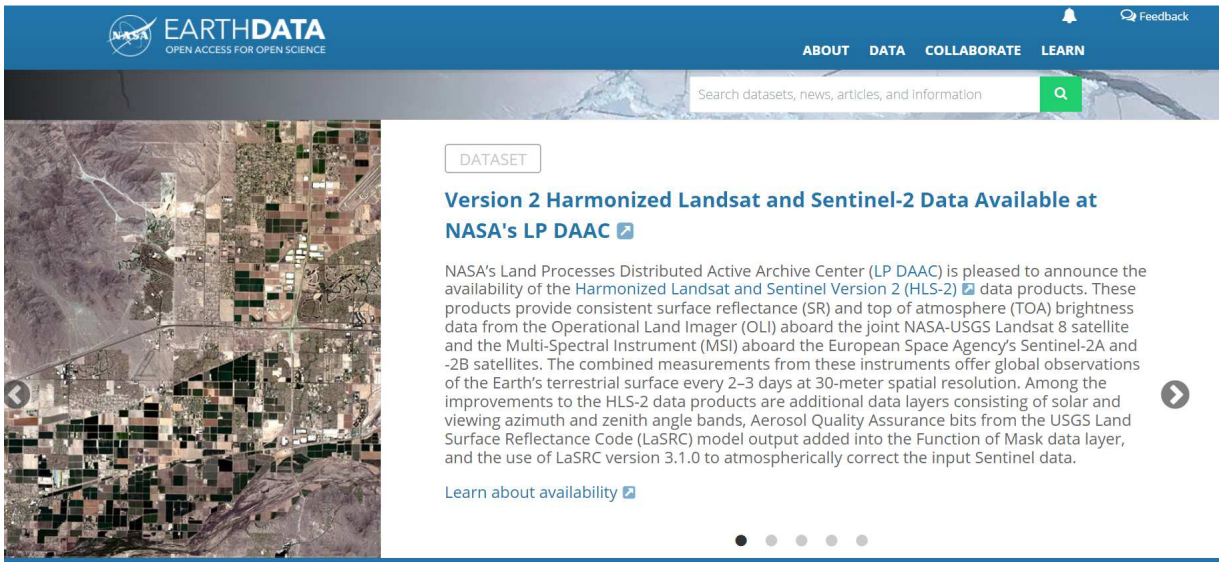

Figure 1: Main Web Page for Earth Data

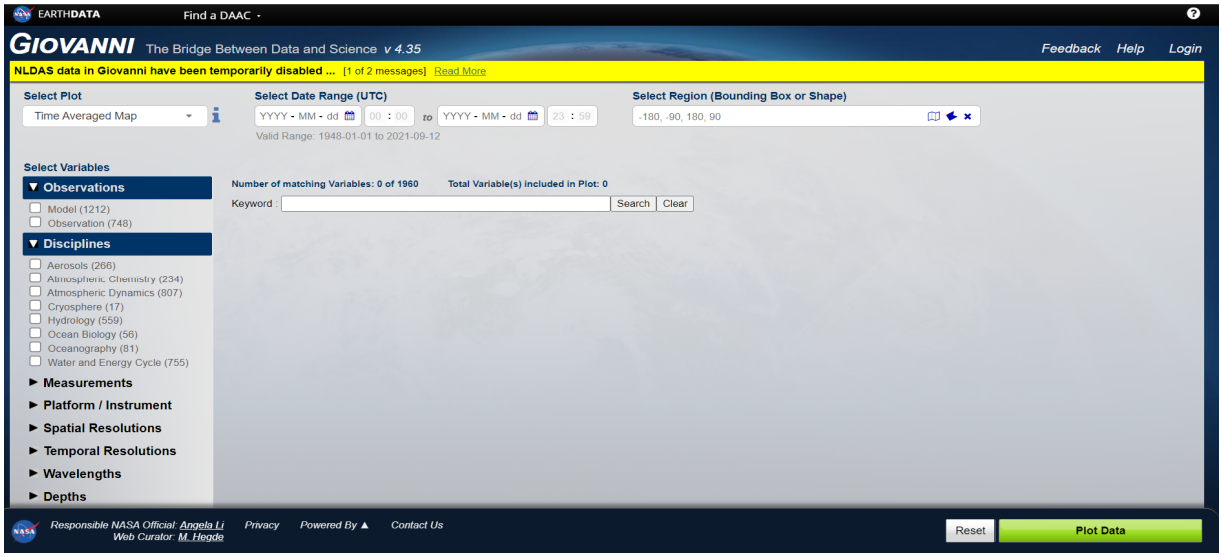

Figure 2: GIOVANNI Application System

The components on this beginning Web page are characterized inside the GIOVANNI system around the world arrangement record. A client can select either the Java or non-Java adaptation. The outcome Web page is one that permits the client to choose the spatial range through the Java picture outline applet or, in case the non-Java adjustment was chosen, physically by entering into an arrangement characterizing a bounding box. The client chooses the transient range of the data as well, one or more parameters from this information set, and the yield type (ASCII or one of some plot sorts). For plots, a couple of color choices are also available. Once the GIOVANNI Web page alternatives are chosen, the client has the alternative of creating a plot or yielding the results to an ASCII record that can be downloaded. The ASCII yield is valuable for Geographic Information Systems (GIS) or other client applications. If plotting is chosen, another Web browser window is opened inside which the plot is shown. Links to the information are given so the client can download the complete information set. Depending upon the parameters chosen, most clients will see the results in a few seconds. For clients who select huge amounts of information either spatially or transiently, the results may take a few minutes. Figure 3 shows the working steps for overall process to verify the data of GIOVANNI system.

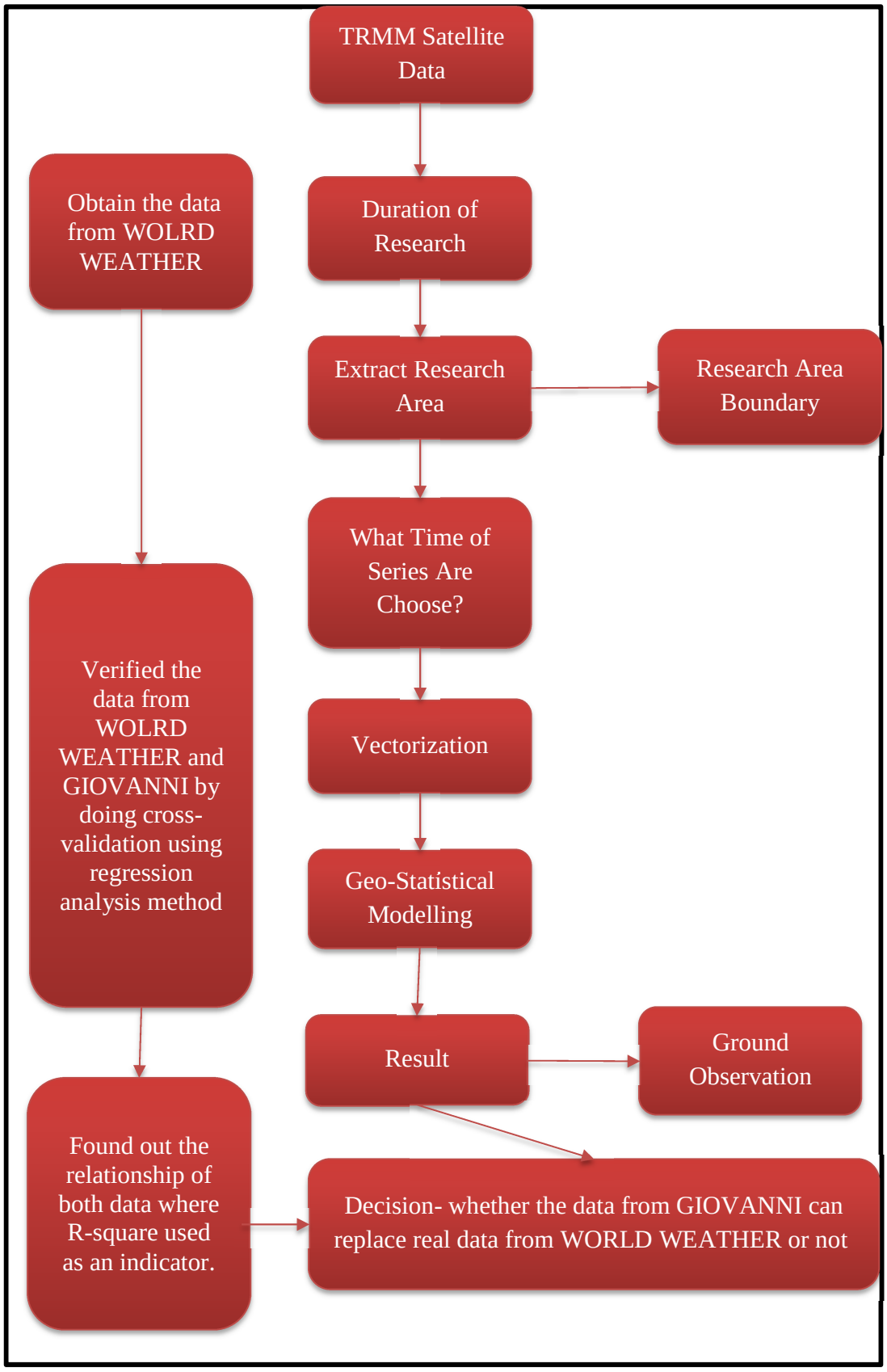

Figure 3: Working Steps for Overall Process

Besides that, TOVAS is used as a sensor in order to measure the rainfall intensity in Penang Island. This sensor provides the user with analysis of the Tropical Rainfall Measuring Mission (TRMM) and a web-based interface for visualization and rainfall intensity on the earth [4]. Figure 4 shows the TRMM precipitation that related instrument.

Instrument name	Band frequencies/ wavelengths	Spatial resolution (km)		Swath width (km)	
		Pre-boost	Post-boost	Pre-boost	Post-boost
Visible and Infrared Scanner (VIRS)	5 channels (0.63, 1.6, 3.75, 10.8, and 12 μm)	2.2	2.4	720	833
TRMM Microwave Imager (TMI)	5 frequencies (10.7, 19.4, 21.3, 37, 85.5 GHz)	4.4 (at 85.5 GHz)	5.1 (at 85.5 GHz)	760	878
Precipitation Radar (PR)	13.8 GHz	4.3 (Vertical: 250 m)	5 (Vertical: 250 m)	215	247
Lightning Imaging Sensor (LIS)	0.7774 μm	3.7	4.3	580	668

Figure 4: TRMM Precipitation That Related Instrument

The frame work for creating the TRMM approximate in real time was created to apply modern concepts in combining quasi-global estimates of rainfall. There are five tools onboard the TRMM satellite and four of them are used to measure rainfall, which are the Visible and Infrared Scanner (VIRS), TRMM Microwave Imager (TMI), Precipitation Radar (PR) and Lightning Imaging Sensor (LIS). Figure 5 shows the working steps of TOVAS sensor

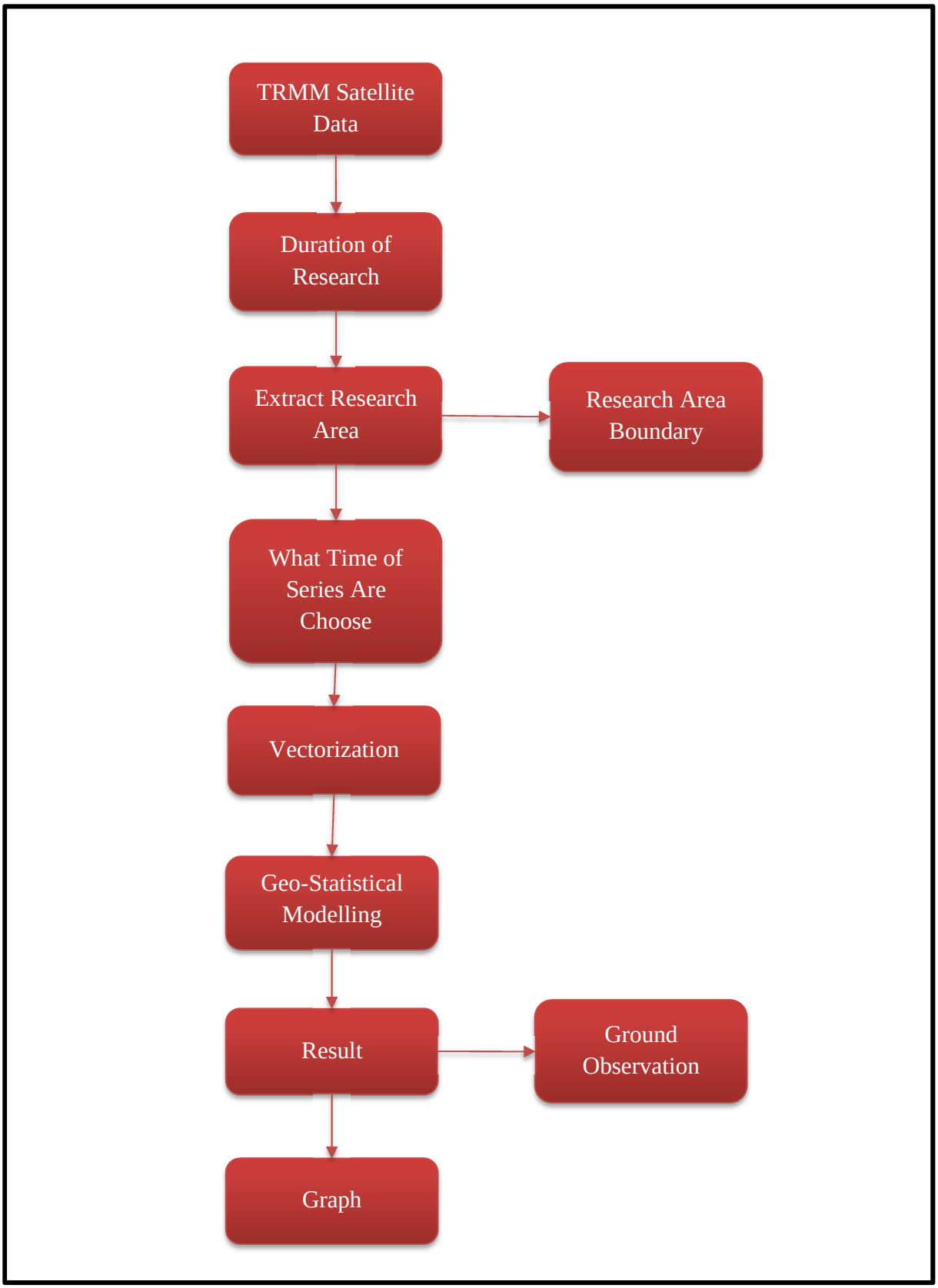

Figure 5: Working Steps Of TOVAS Sensor

2.2 Cross Validation Using Regression Analysis

Cross validation could be a show assessment strategy that's way better than residuals. In order to analyze the data from the GIOVANNI system and WOLRD WEATHER data, cross validation is used to find the relationship between these data by using regression analysis in Microsoft excel. Regression analysis is used to be representative the relationships between a set of independent variables and the dependent variable [11]. Although there are many types of regression analysis, in essence, they all study the influence of one or more independent variables on the dependent variables. Dependent variables are the main factors that should be first to understand or predict, and independent variables are factors that make hypotheses affect dependent variables. In this research, data from the GIOVANNI system is classified as a dependent variable and data from WOLRD WEATHER is an independent variable which represents the Y-axis and X-axis respectively.

Regression analysis produces a regression equation where R-square measures the proportion of variation in the dependent variable that can be attributed to the independent variable [12]. R-squared values range from 0 to 1 and are commonly stated as percentages from 0% to 100%. An R-squared of 100% means that all dependent variables are completely explained by the independent variables, which is higher is better [13]. The R square is also called the coefficient of determination. Multiply R times R to get the R square value. In other words, the coefficient of determination is the square of the coefficient of correlation. In addition, in this research, R-square is obtained by choosing linear trend line as an option. Linear regression is used to estimate the relationship between two quantitative variables, which is to determine how strong the relationship is between two variables. Linear regression is appropriate for modelling linear trends where the data is uniformly spread around the line [14]

3. RESULTS AND DISCUSSION

The following below is the data and result that demonstrates how GIOVANNI was integral to the use of remote sensing data in studying the reliability of GIOVANNI yearly data by comparing with real data from WORLD WEATHER. The both data is compared by doing cross validation using regression analysis where R-square as an indicator to determine whether the relationship between both data is strong or weak, and further shows the accuracy of this system in predicting rain intensity for future event.

3.1 Time Series Monthly Of Rain Intensity for 2016 And 2017

In this section, the rain intensity data was collected to compare with real data. Figure 6 and figure 7 show the time series rain intensity data from WOLRD WEATHER and GIOVANNI systems for the years 2016 and 2017 over the selected region, which is Penang for the period of January 2016 to December 2017. Next, figure 6 shows the highest and lowest time series rain intensity from WOLRD WEATHER, which are 0.1392 and 0.0194 respectively, which were observed in December and March. Then for the GIOVANNI system, the highest and lowest data are 0.5100 and 0.0976 respectively, observed in October and February. It clearly shows different months for the highest and lowest data from both sources.

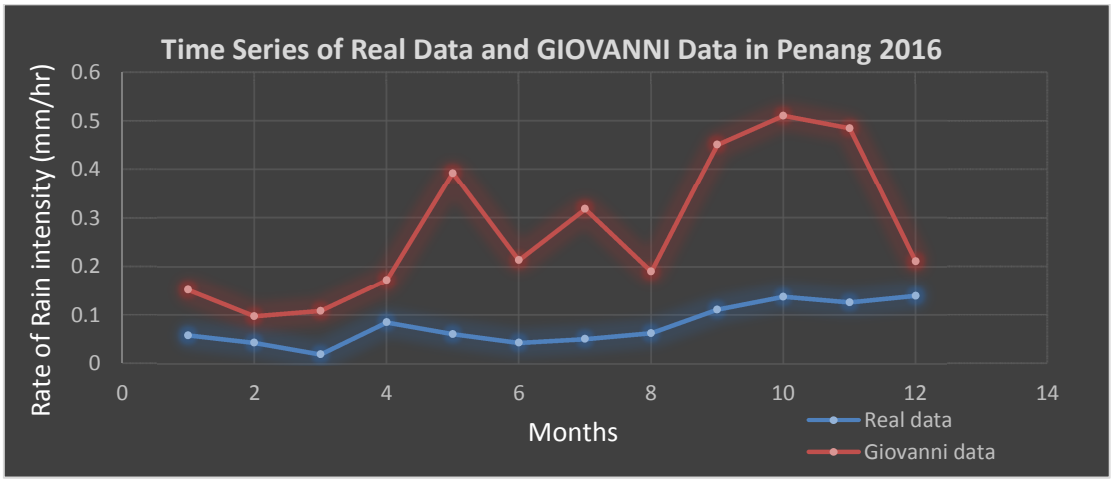

Figure 6: Time Series of Real Data and GIOVANNI Data in Penang 2016

Based on figure 7 below, the highest data for the GIOVANNI system is 0.5683 and the lowest data is 0.1121, which were observed in September and June respectively. Besides that, for the WOLRD WEATHER data, the highest and lowest are 0.2517 and 0.0246 respectively, which were observed in November and July respectively. As with most parts of Malaysia, all year round, Penang gets a tropical climate. It ensures it is warm and humid throughout the year, with little or no weather fluctuations. As stated above, the highest data from the GIOVANNI system and WOLRD WEATHER are in September and November. During these months, it is the wettest months recorded in Penang, with about 21 to 25 days of rainfall. In addition, the lowest data from the GIOVANNI system and WOLRD WEATHER in June and July respectively, where this month the weather is pretty mild with an average of 27 degrees [15]. The sky can be a little greyer in the middle to late afternoons with heavy downpours. So, it makes sense that the highest and lowest data from GIOVNNI accurately suited the climate weather in Penang

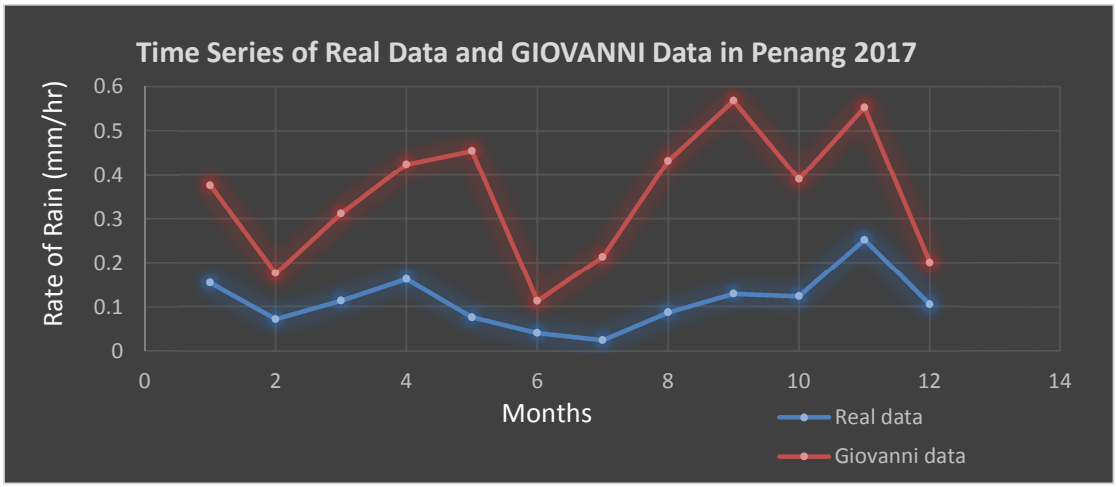

Figure 7: Time Series of Real Data and GIOVANNI Data in Penang 2017

3.2 Result Of Cross Validation by Using Regression Analysis Method

The Regression analysis method is used to verify the data from the GIOVANNI system. The aim of the regression analysis is to determine the parameter values for a function that cause the function to best fit a set of data observations that have been provided [15]. Figure 5 and figure 6 show the regression analysis using excel for data from 2016 and 2017. As stated in both figures, R-square for the data 2016 and data 2017 are 0.4295 and 0.4743 respectively, where R-square is used to measure the strength of the relationship between GIOVANNI data and the WOLRD WEATHER data based on a scale of 0 to 1 [11-14]. A value of 1 means that predictions are similar to the observed values; a value of R-square of more than 1 implies that there is no linear relationship between the observed values and the predicted values. [13, 15].

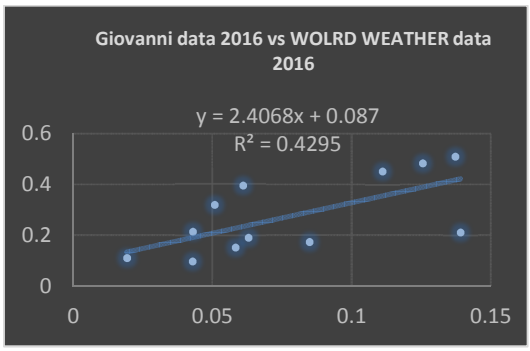

Figure 5: Linear Regression Analysis for 2016 Data

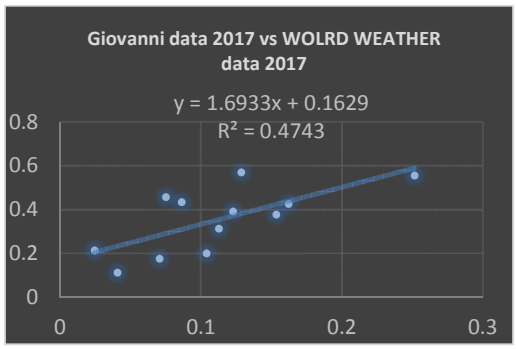

Figure 6: Linear Regression Analysis for 2017 Data

Based on Figures 5 and figure 6, the R-square value is lower than 0.5 where it is considered a weak relationship between data from the GIOVANNI system and WOLRD WEATHER data. [15] A high R-square above 0.60 is needed for research in the field of engineering study. To some degree of accuracy, research may reasonably be predicted. Typically, R-square is at a lower value than commonly agreed for research in the fields of arts, humanities, and social sciences because human behavior cannot be predicted reliably. Therefore, a low R-square is often not an issue in arts, humanities, and social science research. In conclusion, data from satellites using the GIOVANNI system is inaccurate for actual data from WOLRD WEATHER because the relationship between the two data is weak. These data were validated by using regression analysis where R-square as an indicator to decide whether the data relationship is strong or not. In addition, there are several factors that can affect the data from satellites using the GIOVANNI system, such as signal blockage, atmospheric conditions, and others. [16]. For example, the signal blockage is normally affected by weather effects such as snow, ice or heavy to moderate rain, and it can also be influenced by interference from terrestrial sources such as radar, radio relay stations and other nearby transmitting stations.

3.3 Sources Of Error Accuracy Set Data Between Giovanni And World Weather

A first approach to classify inaccuracy real data with remote sensed data which is from GIOVANNI is dividing the sources of error in instrumental errors and environmental conditions.
First source of error is the thematic classification of data. A method to empirically assess the classification accuracy is to select several classes and to compare them with the real data from WORLD WEATHER. By comparing the data sets, the percentage of the pixels correctly classified can be estimated. Pixel refers to the basic unit in an image. From every class representative pixels are selected and compared to the real data. The smaller an area represented by one pixel, the higher the resolution of the image. Here, the main impediment is that large classes have the tendency to be represented by a larger number of points and the small classes may be not represented at all.

Besides that, environmental factors has high possibility affect that accuracy data from GIOVANNI. Some of environments factor such as atmospheric conditions, soil characteristics, vegetation cycles, hydrologic cycles and others. Most of the environmental features are extremely dynamic, in most of the cases the temporal resolution of remote sensed data cannot cover the dynamic domain of the environmental parameters evolution.

Next is instrumental errors which refer to the temporal resolution. Temporal resolution is how often a remote sensing platform collects images of an area which Penang Island. This instruments can be interfered by cloud. Cloud cover often interferes with multi- and hyper-spectral data collection from satellite-based sensors since it masks ground features and it will disturb the accuracy the data from GIOVANNI.

4. CONCLUSION

The GIOVANNI system is a measurement used by many researchers in order to get data from satellites. There are many types of data that can be obtained from satellites through the GIOVANNI system, such as rainfall intensity, aerosol, ocean, and others. Each type of data has its own sensor or instrument in order to get the data. In this research, TOVAS was used as a sensor in order to measure the rainfall intensity in Penang. To find out the reliability of the data of the GIOVANNI system, cross validation of data by using regression analysis is conducted. R-square is an indicator used to measure how strong the relationship between the data from the GIOVANNI system is with real data from WOLRD WEATHER. Based on the results, the data from the GIOVANNI system is inaccurate and should be replaced with real data like WOLRD WEATHER because the relationship between the two data is weak. GIOVANNI data was validated using regression analysis where R-square as an indicator to determine whether the relationship between the two data is strong or weak, which is below 0.5 is considered weak data. According to R-square for 2016 and 2017, 0.4295 and 0.4743 respectively.

ACKNOWLEDGEMENTS

The authors would like to express gratitude for the support given by the Faculty of Chemical Engineering, Universiti Teknologi MARA, Cawangan Pulau Pinang and Final Year Project (FYP) Coordinator for their helps and constructive comments in the preparation of the final year project paper.

5. REFERENCES

1. Risdiyanto, Syaripin (2021) Study of Saturation Flow at Signalized Intersection on Sunny Weather and Rainy Weather. In: Mohammed B.S., Shafiq N., Rahman M. Kutty S., Mohamad H., Balogun AL. (eds) ICEE2020. IC CODE 2021. Lecture Notes in Civil Engineering, vol 132. Springer, Singapore.
2. Wesström, I., Messing, I., Linner, H., & LindstroÈm, J. (2001). Controlled drainage effects on drain outflow and water quality. Agricultural water management, 47(2), 85-100.
3. Ismail, W. R. (1995). The impact of hill land clearance and urbanisation on hydrology and geomorphology of rivers in Pulau Pinang, Malaysia. The University of Manchester (United Kingdom).
4. Liu, J., Bray, M., & Han, D. (2012). Sensitivity of the Weather Research and Forecasting (WRF) model to downscaling ratios and storm types in rainfall simulation. Hydrological Processes, 26(20), 3012-3031.
5. Chan, N. W. (1997). Increasing flood risk in Malaysia: causes and solutions. Disaster Prevention and Management: An International Journal.
6. Tan, M. L., Samat, N., Chan, N. W., Lee, A. J., & Li, C. (2019). Analysis of precipitation and temperature extremes over the Muda River Basin, Malaysia. Water, 11(2), 283.
7. Zhang, X., Chen, N., Chen, Z., Wu, L., Li, X., Zhang, L., & Li, D. (2018). Geospatial sensor web: A cyber-physical infrastructure for geoscience research and application. Earth-science reviews, 185, 684-703. 8
8. A. Werkmeister, M. Lockhoff, M. Schrempf, K. Tohsing, B. Liley and G. Seckmeyer, Atmos. Meas. Tech., 2015, **8**, 2001–2015.
9. Drusch, M., Del Bello, U., Carlier, S., Colin, O., Fernandez, V., Gascon, F., ... & Bargellini, P. (2012). Sentinel-2: ESA's optical high-resolution mission for GMES operational services. Remote sensing of Environment, 120, 25-36.
10. Peterson, R. A., & Cavanaugh, J. E. (2019). Ordered quantile normalization: a semiparametric transformation built for the cross-validation era. Journal of Applied Statistics.
11. Marrie, R. A., Dawson, N. V., & Garland, A. (2009). Quantile regression and restricted cubic splines are useful for exploring relationships between continuous variables. Journal of clinical epidemiology, 62(5), 511-517.
12. Kumari, S. S. (2008). Multicollinearity: Estimation and elimination. Journal of Contemporary research in Management, 3(1), 87-95.
13. Chicco, D., Warrens, M. J., & Jurman, G. (2021). The coefficient of determination R-squared is more informative than SMAPE, MAE, MAPE, MSE and RMSE in regression analysis evaluation. PeerJ Computer Science, 7, e623..
14. Beale, C. M., Lennon, J. J., Yearsley, J. M., Brewer, M. J., & Elston, D. A. (2010). Regression analysis of spatial data. Ecology letters, 13(2), 246-264.
15. Wouthuyzen, S., Abrar, M., & Lorwens, J. (2018, February). A comparison between the 2010 and 2016 El-Ninō induced coral bleaching in the Indonesian waters. In IOP Conference Series: Earth and Environmental Science (Vol. 118, No. 1, p. 012051). IOP Publishing.
16. Chini, P., Giambene, G., & Kota, S. (2010). A survey on mobile satellite systems. International Journal of Satellite Communications and Networking, 28(1), 29-57.

THE STUDY OF INTERACTIONS BETWEEN MWCNT-OH, MWCNT-COOH, AND MWCNT-COCl WITH METHYLENE BLUE VIA DENSITY FUNCTIONAL THEORY

Nashita Aliah Fahira Ahmad Fadzil[1] and Marina Mokhtar[2,*]
[1]Faculty of Chemical Engineering, Universiti Teknologi MARA, Cawangan Pulau Pinang, 13500 Permatang Pauh, Pulau Pinang, Malaysia
[2]Faculty of Applied Sciences, Universiti Teknologi MARA, Cawangan Pulau Pinang, 13500 Permatang Pauh, Pulau Pinang, Malaysia
(*email: mmarina@uitm.edu.my)

ABSTRACT- The adsorption of methylene blue (MB) onto multi-walled carbon nanotubes (MWCNTs) membrane has been the latest technology in dye removal. The purpose of this study was to examine the interaction between MWCNT-OH, MWCNT-COOH, and MWCNT-COCl with MB by using the density functionalized theory (DFT) method, as preliminary work. The calculation has been done through Gaussian 03 software packages. This method used B3LYP with 6-31G(d) as a basis set for geometry optimization. The basis set 6-31+G(d) was used for energy calculations. As a result, the simulation of MB with MWCNT-OH, MWCNT-COOH, and MWCNT-COCl showed an electrostatic attraction and hydrogen bonding as the main interaction in the adsorption. In conclusion, the interaction between MB and MWCNT-OH is strongest with the preferred distance is at 1.36 Å. The calculation by the DFT method is a good computational method to do the preliminary study, where it can show the good absorbent before run the laboratory works on the wastewater treatment.

Keywords: methylene blue, density functional theory, adsorption, multi-walled carbon nanotubes.

1. INTRODUCTION

Computational chemistry is a part of theoretical study, and it is commonly used in medicinal manufacturing to discover the relations of biomolecules with potential drugs. Computational chemistry consists of five broad classes: molecular dynamics, density functional theory, semi-empirical, ab initio, and molecular mechanics calculations [1, 2] and can calculate relative energies and geometries with high accuracy because of the built-in correlation [2]. DFT is commonly used for large molecules because it can calculate fast and appear to be more basis-set-saturated than the ab initio and other methods.

Over the years, multi-walled carbon nanotubes (MWCNTs) have gained great attention due to their ability to work as effective adsorbents for biological and chemical contaminants. The usage of MWCNTs to eliminate contaminants has created good interest due to the natural characteristics such as hollow and porous structures, ease of implementation of new functional groups, chemical, mechanical, and radiation stability, high thermal, large surface area, and lightweight density [3–5]. MWCNTs were made from graphene that makes it naturally a hydrophobic material. The hydrophobic property can be altered by attached functional groups such as hydroxyl, sulfate, or chloride in order to make the nanomaterial optimize its function. The strong interaction between functionalized MWCNTs with organic dyes can be an indicator that

the strong adsorption, thus makes the nanocomposite material a good absorbent in wastewater treatment.

Dyes are the essential colored materials that are extensively used for numerous industrial processes such as coatings, detergents [4], textiles, leather, paper, rubber, printing, plastics [5], carpets [6], and cosmetics [7]. The existence of dyes in effluent causes main water contamination problems due to the direct discharge of dyes from industrialization into streams [3–7]. The presence in water of even minimal quantities of dyes, less than 1 ppm for certain dyes, is easily recognizable and unacceptable [8].

The hydrophobic property of CNTs is indispensable for the adsorption of aromatic contaminants like benzene and anthracene. In this study, the density functional theory of selected functionalized MWCNTs as adsorbents of methylene blue (MB) is carried out. This study aims to determine the interaction of selected functionalized MWCNTs using the density functional theory method and the lowest energy formed between selected functionalized MWCNTs with MB.

2. EXPERIMENTAL DETAIL

DFT was calculated using Gaussian 03 software package [9]. The simulation can be performed in three stages: preparation and optimization, build the complex molecules absorbent-absorbate, and calculation.

Stage 1: Preparation of molecules

MWCNTs structure was built using a nanotube modeler software [10]. The structure containing 30 carbon atoms, a (3,3) chiral index, 5 Å tube length, and 1.421 Å bond length. The surfaces of MWCNTs were attached to functional groups such as hydroxyl (-OH), the carboxylic acid (-COOH), and acyl chloride (-COCl), respectively [11]. The structure of methylene blue (MB) was draw using Gaus View 4.0v [12]. Both MWCNT-OH, MWCNT-COOH, MWCNT-COCl, and MB were optimized using Gaussian 03. Figure 1 shows the structure of the molecules.

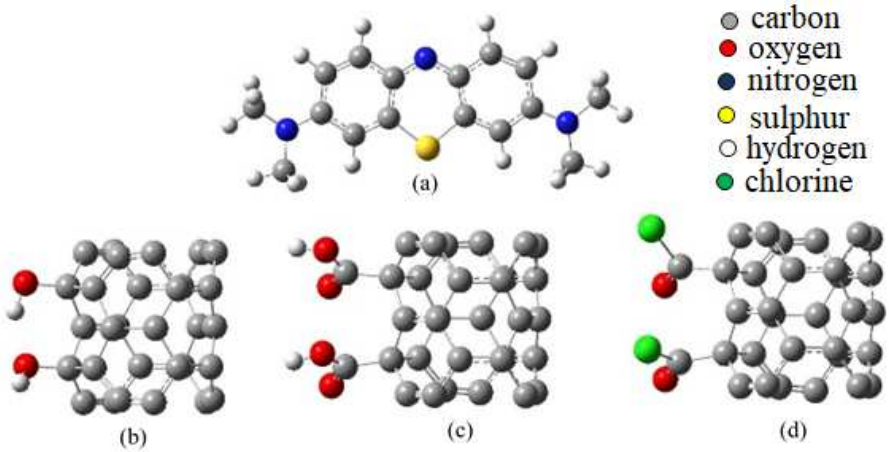

Figure 1. Optimized DFT structures of (a) MB, (b) MWCNT-OH, (c) MWCNT-COOH and (d) MWCNT-COCl

Stage 2: Complex molecules development

A complex between each MWCNT-OH, MWCNT-COOH, MWCNT-COCl with MB was develop using Gaussian 03. Each functionalized MWCNTs was put near the MB structure at the distance of 0.8 Å, 1.36 Å, and 2.0 Å. The distance was based on the average range of van der Waals forces, dipole-dipole forces, and hydrogen bonds [13], where interaction is perceived to take place either by coordination or electrostatic attraction [11].

Stage 3: Calculation and analysis

The Gaussian 03 calculation setup used energy at the Becke three-parameter Lee Yang Parr (B3LYP) functional with 6-31G (d) to do the calculations. It was used as the basis set to produce the stable conformation, reducing the system's energy and altering the molecular geometry [14]. While for energy calculations, the B3LYP method with 6-31+G(d) basis set is used. The manipulated variables in the calculations are the distance between optimized MB and functionalized MWCNTs. The results from the DFT calculations were used to analyze the electronic properties.

3. RESULTS AND DISCUSSION

3.1 Intermolecular forces

The electronic properties for each of the MWCNT-OH, MWCNT-COOH, MWCNT-COCl with MB were analyzed using the data collected at the output of the simulation. The MB molecule is a cationic dye with a positive charge that binds it to a negatively-charged molecule [15]. MB has C-C double bonds and contains π-electrons that make it positive in aqueous media [16]. MWCNT-OH and MWCNT-COOH are negatively charged molecules, while MWCNTs-COCl is a polar molecule with dipole-dipole attractions between its molecules and van der Waals dispersion forces.

The adsorption of MB is classified as physisorption, which is physical adsorption. When MB is close to MWCNT-OH, MWCNT-COOH, and MWCNT-COCl, the positively charged nitrogen (N) in the MB molecule will attract negatively charged oxygen (O) in the molecules with a certain distance. Results showed that the interaction of MB-MWCNT-OH and MB-MWCNT-COOH are at the average bond length of 1.36 Å. The interaction between MB and MWCNTs-COCl formed an average bond length of 1.611 Å. The bond lengths give an indication of the bond strength. The result showed that the interaction in the complexes of MB-MWCNT-OH and MB-MWCNT-COOH are stronger compared to the MWCNTs-COCl.

The mechanism of MB adsorption on functionalized MWCNTs may be explained by several forms of interactions, as described in the literature [17]. Commonly, there are three types of interaction formed in the complex namely H-bonding, electrostatic, and π-π interaction. The illustration of the interaction formed between absorbent and absorbate can be shown in figure 2. In the reaction, the absorbent formed a negative ion because it has hydroxyl, carboxylate, or acyl chloride functional group, and MB is a positive ion, which has a positively charged N^+ group.

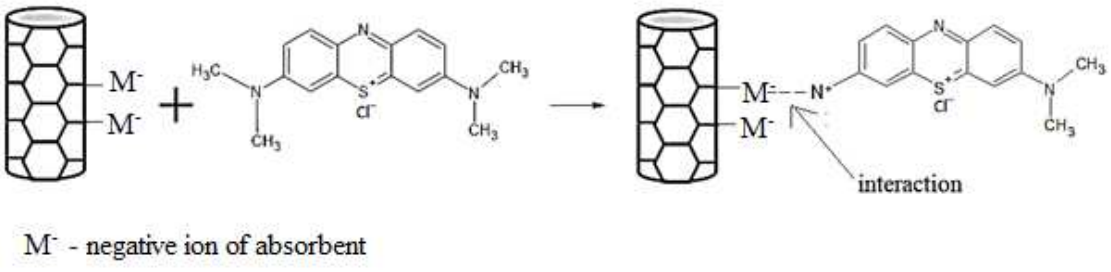

Figure 2. The interaction between MB and functionalize MWCNT.

3.2 Comparison of energies

Intermolecular forces between negative ion of absorbent and nitrogen ion in methylene blue can be recognized by the value of formation energy calculated in the simulation. The formation energy calculated from the simulation can be used as a preliminary study to recognize the type of interactions. Table 1 shows the value of formation energy when the interaction is formed in the simulation. It shows that the energy obtained from the interaction of MB with MWCNT-OH, MWCNT-COOH, and MWCNT-COCl has a large difference from each other. The more negative the energy is, the stronger the interaction between the MB and functionalized MWCNTs. Table 1 demonstrates a larger negative value of energy between MB and MWCNT-COCl than for MWCNT-OH and MWCNT-COOH. This is due to the electronegative properties of the chlorine atom in MWCNT-COCl that pulls electrons toward it in the C-Cl. The Cl- is an excellent leaving group which makes the replacing step fast. The interaction between MB and MWCNTs-COOH has a large negative energy value than for MWCNT-OH. This is because the MWCNT-COOH molecule can form hydrogen bonding and the presence of two oxygen atoms in the molecule makes it more electronegativity. Among all the selected functional groups, MWCNT-COOH is the most polar functional group because it has two electronegative atoms, has a dipole moment, and can hydrogen bond extensively compared to MWCNT-OH and MWCNT-COCl.

Table 1: The energy value for the formation of interaction in MWCNT-OH, MWCNT-COOH, and MWCNT-COCl.

Interaction between adsorbents - absorbate	Energy (a.u)
MB-MWCNT-OH	-2474.3715
MB-MWCNT-COOH	-2701.4664
MB-MWCNT-COCl	-3471.2873

The interaction of MB and MWCNT-OH, MWCNT-COOH, MWCNT-COCl were analyzed according to the distance and energy obtained from the energy calculations. Different distance gives a different kind of energy value. Figure 3 shows the effect of distance on the energy of interaction between MB and MWCNTs-OH. Figure 3 illustrates that the distance between MB and MWCNT-OH at 0.8 Å was -2470.83 a.u, while at 1.36 Å distance, the energy value was -2474.37 a.u which is lower than the previous distance. Then, the energy rose to -2470.06 a.u at a distance of 2.0 Å. This shows that the energy at distance 1.36 Å was the larger negative energy value between MB and MWCNT-OH.

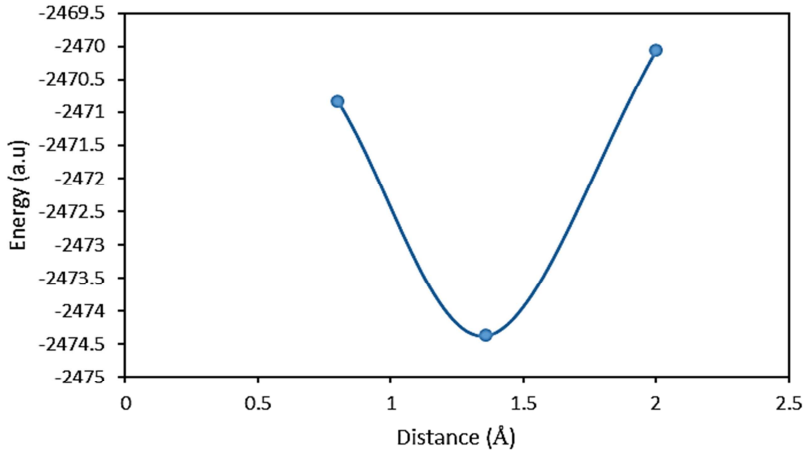

Figure 3: Effect of distance on the energy of interaction between MB and MWCNT-OH

Figure 4 demonstrates the effect of distance on the energy of interaction between MB and MWCNT-COOH. As shown in Figure 4, the first distance between MB and MWCNT-COOH was 0.8 Å, followed by 1.36 Å and 2.0 Å. The energy value for distance 0.8 Å was -2698.34 a.u, while for distance 1.36 Å, the energy value was -2474.37 a.u which shows a slight decrease from the previous value. The energy value for distance 2.0 Å was decreasing to -2470.06 a.u, which shows the larger negative energy value between MB and MWCNT-COOH.

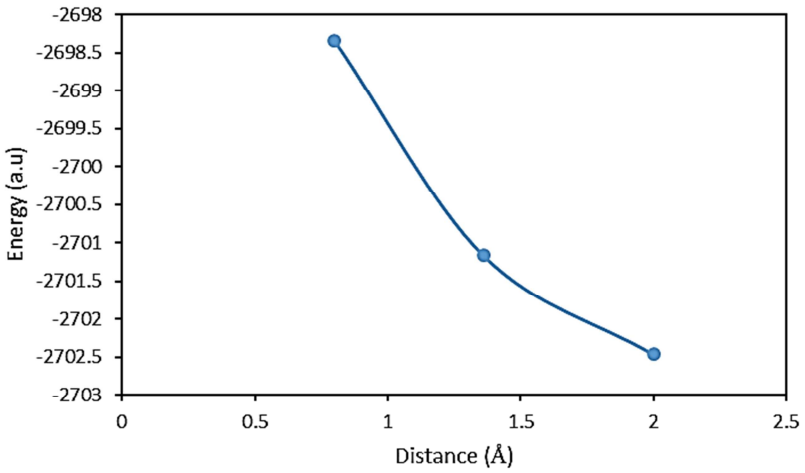

Figure 4. Effect of distance on the energy of interaction between MB and MWCNT-COOH

Figure 5 shows the effect of distance on the energy of interaction between MB and MWCNTs-COCl.Based on Figure 5, as mention before, the closest distance for interaction between MB and MWCNT-COCl was 0.845 Å. The energy value for distance 0.845 Å was -3467.9602 a.u. Meanwhile, for distance 1.611 Å, the energy value was -3470.55 a.u, and for distance 2.377 Å, the energy value was -3471.29 a.u. The larger negative energy value for interaction between MB and MWCNT-COCl was at a distance of 2.377 Å.

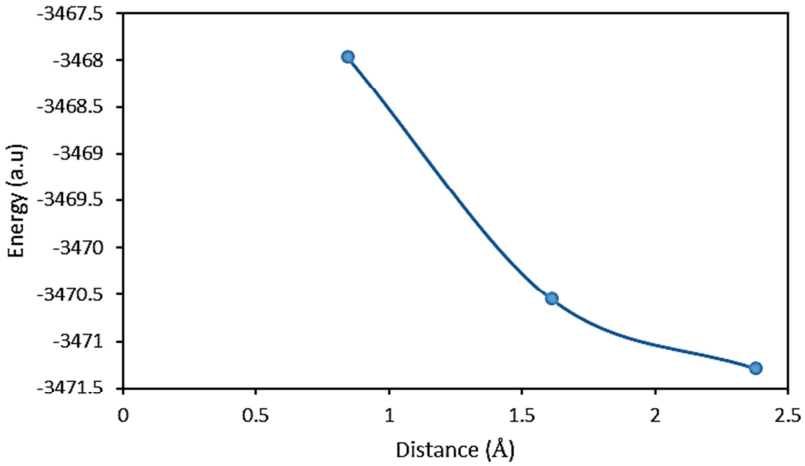

Figure 5: Effect of distance on the energy of interaction between MB and MWCNT-COCl

The selective interaction for MB with MWCNT-OH, MWCNT-COOH, and MWCNT-COCl was at distances 1.36 Å, 2.0 Å, and 2.377 Å, respectively. The energy value at these distances was the larger energy value compared to other distances. The more negatives these values are, the stronger the interaction between MB and functionalized MWCNTs. This indicates strong chelating interaction between MB and functionalized MWCNTs.

4. CONCLUSION

The study of density functional theory on MWCNT-OH, MWCNT-COOH, MWCNT-COCl as adsorbents of methylene blue can be used as a preliminary study to examine the interaction between them. All three complexes showed that electrostatic interaction and H-bonding are the main interaction in the absorption. The computational method also showed that MWCNT-OH can be a better absorbent compared to the other two because of the shortest distance (1.36 Å) between MB and MWCNT-OH, and the distance is the preferred distance as it showed the lowest energy when MB absorption onto the MWCNT-OH surface.

ACKNOWLEDGEMENT

The author are grateful to the Universiti Teknologi MARA Cawangan Pulau Pinang, Faculty of Chemical Engineering for the physical and technical supported in this work.

5. REFERENCES

1. E. Lewars, *Introd. to theory Appl. Mol. quantum Mech.* 318 (2011).
2. G. L. Patrick, *An introduction to medicinal chemistry*, Oxford university press (2013).
3. N. X. Dinh, T. Q. Huy, and A.-T. Le, *J. Sci. Adv. Mater. Devices* 1, 84 (2016).
4. Y. Zhou, J. Lu, Y. Zhou, and Y. Liu, *Environ. Pollut.* 252, 352 (2019).
5. Y. Bulut and H. Aydın, *Desalination* 194, 259 (2006).
6. D. Özer, G. Dursun, and A. Özer, *J. Hazard. Mater.* 144, 171 (2007).
7. N. Boukhalfa, M. Boutahala, N. Djebri, and A. Idris, *J. Mol. Liq.* 275, 431 (2019).
8. M. Rafatullah, O. Sulaiman, R. Hashim, and A. Ahmad, *J. Hazard. Mater.* 177, 70 (2010).
9. J. A. . Frisch, M. J.; Trucks, G. W.; Schlegel, H. B.; Scuseria, G. E.; Robb, M. A.; Cheeseman, J. R.; Montgomery, Jr., J. A.; Vreven, T.; Kudin, K. N.; Burant, J. C.; Millam, J. M.; Iyengar, S. S.; Tomasi, J.; Barone, V.; Mennucci, B.; Cossi, M.; Scalmani, G.; R, Gaussian 03, Revision C.02, (2004).
10. M. Yoshida, Nanotube modeler, (2018).at <http://www.jcrystal.com/products/wincnt/index.htm>
11. O. A. Oyetade, A. A. Skelton, V. O. Nyamori, S. B. Jonnalagadda, and B. S. Martincigh, *Sep. Purif. Technol.* 188, 174 (2017).
12. A. Frisch, R. I. I. Dennington, T. Keith, J. Millam, A. B. Neilsen, and A. J. Holder, *Inc. Pittsburg, PA* (2007).
13. M. J. Minch, An introduction to hydrogen bonding (Jeffrey, George A.), (1999).
14. T. N. V. de Souza, S. M. L. de Carvalho, M. G. A. Vieira, M. G. C. da Silva, and D. do S. B. Brasil, *Appl. Surf. Sci.* 448, 662 (2018).
15. M. E. L. Alouani, S. Alehyen, M. E. L. Achouri, and M. Taibi, *J. Mater. Environ. Sci.* 9, 32 (2018).
16. A. Ghaffar and M. N. Younis, *Green Process. Synth.* 4, 209 (2015).
17. R. Saxena, M. Saxena, and A. Lochab, *ChemistrySelect* 5, 335 (2020).

SAFETY PRACTICES ON WASTE DISPOSAL IN ACADEMIC LABORATORIES AMONG LABORATORY STAFF

Nor Aimi Abdul Wahab[1], Farah Nabilah Ahmad Rahiza[2], Nur Maizatul Azra Mukhtar[3], Marina Mokhtar[4]
[1,4] *Department of Applied Sciences,Universiti Teknologi MARA, Cawangan Pulau Pinang, Kampus Permatang Pauh*
**noraimi108@uitm.edu.my, mmarina@uitm.edu,my*
[2] *School of Chemical Engineering, College of Engineering, Universiti Teknologi MARA, Cawangan Pulau Pinang, Kampus Permatang Pauh*
Farahiza31@gmail.com
[3] *Fakulti Sains Kesihatan, Universiti Teknologi MARA, Cawangan Pulau Pinang, Kampus Bertam*
nurmaizatul038@uitm.edu.my

ABSTRACT- Academic laboratories are considered a potentially hazardous workplace. Several laboratory accidents have been reported worldwide in laboratories of higher education and research institution with catastrophic consequences. These laboratories accidents may be caused by the use of various types of hazardous substances and material, improper disposal of laboratory waste, specialised equipment, lack of safety compliance, and poor safety culture. Therefore, safety practice and a strong safety culture must be of utmost importance in the academic laboratories among laboratory staff as failure in implementing safety could lead to injuries. Thus, this study aims to identify the safety practices of the laboratory staff in the university, focusing on the waste disposal process in the academic laboratories using a laboratory safety questionnaire. The questionnaire was distributed online to laboratory staff (N=50) for two weeks. The analysis was based on 23 item close-ended questionnaires grouped in the following categories: demographics (7), knowledge on waste management (3), laboratory waste management (5), laboratory safety practices (3) and personal protective equipment (PPE) and emergency responses (5) with a total of 50 respondents participated in this study. For self-perceived risk, only 44 % of the respondents felt exposed to a high and very high level of risk from work conducted in the laboratory. It was found that the safety practices among laboratory staff focusing on waste disposal is satisfactory with evaluations conducted on knowledge on waste management, laboratory waste management, laboratory safety practices and PPE and emergency responses. However, the safety practices among laboratory staff could be further improved by ensuring all laboratory staff attend safety training and implement a safety model comprising safety culture and practices with the organisational commitment to create a safe workspace in the laboratory.

Keywords: Safety, Practices, Waste Disposal, Academic Laboratory, Laboratory Staff

1. INTRODUCTION

Academic laboratories are considered a potentially hazardous workplace. Many laboratory accidents have been reported worldwide in laboratories of higher education and research institutions with catastrophic consequences [1]. These laboratories accidents may be caused by the use of various types of hazardous substances and materials, improper disposal of laboratory waste, specialized equipment, lack of safety compliance, and poor safety culture [1]. One of the main activities in the academic laboratory is the management of waste disposal. Proper waste management and waste disposal are essential to maximize safety and minimize environmental impact. According to [2],

academic laboratories are more dangerous than industrial laboratories due to the less stringent safety management/culture and lower safety investment in academic laboratories compared to industrial laboratories. The occurrence of accidents in academic laboratories has been underestimated, where it is reported that there are 10 to 50 times more accidents in academic laboratories than in industrial laboratories [3]. Based on the research data, many academic laboratories management have realized the need for laboratory safety as a top priority. Therefore, safety practice and a strong safety culture must be of utmost importance in the academic laboratories among laboratory staff. Failure in safety practice among laboratory staff can seriously affect laboratory users as they are exposed to various hazards, which could cause injuries and could badly affect the efficiency of the laboratory and disturb the learning process [4]. An online survey conducted within a medium-sized Canadian University shows a lack of strong and positive safety culture and safety compliance within the university laboratory[1]. A research carried out by [3] to establish the relationship between accidents in academic laboratories, and the institution safety climate at several public higher education institutions in Northwest Mexico revealed that the absence of institutional safety commitments contributes to an increased accident in laboratories. It shows that academic laboratories must implement a safety culture where laboratory staff must practice a positive safety culture and good laboratory safety practices to prevent accidents. However, academic lab safety research is still underdeveloped and there is limited data on laboratory staff attitudes and behaviors especially dealing with laboratory waste [5]. Thus, this study aims to identify the safety practices of the laboratory staff, focusing on the waste disposal process in the academic laboratory.

2. EXPERIMENTAL DETAILS

2.1 Sample Collection

A cross-sectional study was conducted to determine the safety practices on waste disposal among laboratory staff in the academic laboratory. The study was conducted using a laboratory safety questionnaire adapted from [1][2]. The questionnaire was distributed online to laboratory staff within two weeks. Samples were collected using convenience sampling with inclusion criteria of staff working in the laboratory with at least one year of working experience in the laboratory. A total of 50 (N=50) laboratory staff participated in this study.

2.2 Questionnaire survey

The questionnaire was distributed to participants through an online platform. The questionnaire was based on 23 item close-ended questionnaires grouped in the following categories: demographics (7), knowledge on waste management (3), laboratory waste management (5), laboratory safety practices (3), personal protective equipment (PPE) and emergency responses (5). The knowledge section required a yes or no answer, while the rest of the item was based on a five-point Likert scale.

2.2 Data analysis

The collected data were descriptively analysed, and the result was depicted in frequency distribution tables expressed in percentage.

3. RESULTS AND DISCUSSION

A total of 50 individuals participated in this study. The majority of the respondents were female in the age group of 35 – 54 years. 32.7 % of the respondents have 1-5 years of working experience in a laboratory setting, while only 9.6 % have more than nine years of working experience. The majority of the respondents possess master's degree qualifications. For the self-perceived level of risk, 44 % of respondents felt that their level of risk from work conducted at the laboratory was high and very high, 30 % moderate, and 26% low to very low, as shown in Table 1. The result is in contrast with the study by [1], where 59% indicated that the level of risk associated with their laboratory work was low or very low. The results suggest that most of the participants in this study are aware of their risk while conducting work in the laboratory. However, more awareness should be given to the staff on the risk they face in the laboratory to ensure that the self-perceived risk could be improved.

Regarding training on chemical waste management, 68 % of the respondents agree that they have received training on chemical waste management, which means they are aware of the waste management procedure. The remaining 32 % of respondents have not received training on chemical waste management, leading to improper laboratory waste disposal. Thus, the laboratory management needs to conduct training on laboratory waste among the staff on a timely basis. According to [6], it is essential to train workers and students to standardize waste disposal procedures. It could be a platform for sharing information on the waste disposal process and new regulations.

Table 1: Self-perceived risk

Category	Sub-category	Response frequency
Self-perceived level of risk of the work conducted in the laboratory	Low to very low	26%
	Moderate	30%
	High to Very High	44%
I received training or workshop regarding chemical waste management	Yes	68%
	No	32%

Three items were evaluated on the knowledge of waste disposal: categorizing chemical waste, type of container use, and labeling of chemical waste. The result is depicted in Table 2. 80 % of the respondents agree that they know how to categorize waste, 76 % know the suitable container to use, and 68 % know how to label the chemical waste. The leading cause of the accident in the university laboratory is improper storage of chemicals, inappropriate use of chemicals, and improper chemical disposal [7]. Thus, this knowledge on laboratory waste management is essential to ensure proper and correct laboratory waste disposal is practiced in the laboratory.

Table 2: Knowledge on waste management

Category	Sub-category	Response frequency
I know how to categorized chemical waste	Yes	80%
	No	20%
I know the type of container that is compatible with the chemical waste	Yes	76%
	No	24%
I know how to label the chemical waste	Yes	68%
	No	32%

Practice on laboratory waste management in the laboratory is shown in Table 3. 72% of participants agree that the laboratory waste is being stored in compatible containers and is clearly labeled according to the type of the waste. 78% of respondents agree that Standard Operating Procedure (SOP) is provided for waste disposal. The SOP is essential to serve as a guideline for laboratory users for the waste disposal process as different categories of waste require different processing procedures. The SOP should include procedures on the correct segregation and processing of laboratory waste. It would act as guidance on how to dispose of hazardous waste [9] properly. 74 % of laboratory staff agree that all expired chemical is disposed of according to the SOP of waste disposal. However, 22 % of respondents neither agree nor disagree with this statement. It could be improved by having the SOP in the form of a chart posted on the laboratory wall for fast and easy reference of the laboratory staff and having refresher training at least once a year.

On the inventory of laboratory waste, 6% of the respondents disagree that the inventory for categories and quantities of laboratory wastes generated, treated and disposed of is accurate and up-to-date. Having an accurate and up-to-date inventory is essential to ensure the waste is appropriately managed and help minimize how much waste is stored onsite and provide hazard and safety information, which is essential in planning and implementing laboratory procedures. Having an e-inventory database in the laboratory could help increase efficiency, improve accuracy and help to keep up-to-date information. [8] developed a chemical management system (CMS) an inventory management software at Sandia National Laboratories. The use of this system help management of chemical inventory by providing the information and hazard of the chemical so that institution are better prepared in terms of safety and protecting laboratory users.

Table 3: Laboratory waste management practice

Category	Sub-category	Response frequency
The laboratory waste is being stored in compatible containers	Strongly agree	34%
	Agree	38%
	Neutral	26%
	Disagree	2%
	Strongly disagree	0%
Containers of laboratory wastes are clearly labelled by the types applicable to them	Strongly agree	38%
	Agree	34%
	Neutral	20%
	Disagree	8%
	Strongly disagree	0%
Standard Operating Procedure (SOP) is provided for waste disposal	Strongly agree	36%
	Agree	42%
	Neutral	22%
	Disagree	0%
	Strongly disagree	0%
All expired chemical is disposed of according to the Standard Operating Procedure (SOP) of waste disposal	Strongly agree	38%
	Agree	36%
	Neutral	26%
	Disagree	0%
	Strongly disagree	0%
The inventory for categories and quantities of laboratory wastes generated, treated and disposed of is accurate and up-to-date	Strongly agree	34%
	Agree	28%
	Neutral	32%
	Disagree	6%
	Strongly disagree	0%

The result on laboratory safety practices among laboratory staff is given in Table 4. For laboratory safety practices, 86% of the participants claimed that they properly segregate all laboratory waste. The high percentage of compliance on waste segregation may be due to having an SOP on waste disposal prepared by the laboratory management. 70 % of the respondents revealed that all accident is recorded in the accident record book. All laboratory staff must record the details of any accidents that occur in the laboratory so that proper action can be taken to prevent future accidents from happening. Lastly, only 76% of the participants agreed that Safety Data Sheets (SDS) for all chemicals are provided in their laboratory. It is of utmost importance to ensure that all SDS is provided in the laboratory as it holds information on managing the risk of chemical handling in the workplace. The laboratory staff must ensure that all chemicals come with SDS. Having a digital SDS database will help improve SDS management and provide easier and faster access to SDS.

Table 4: Laboratory safety practices

Category	Sub-category	Response frequency
I properly segregate all laboratory waste	Strongly agree	48%
	Agree	38%
	Neutral	10%
	Disagree	4%
	Strongly disagree	0%
All accident is recorded in the accident record book	Strongly agree	34%
	Agree	36%
	Neutral	26%
	Disagree	2%
	Strongly disagree	2%
Safety Data Sheets (SDS) for all chemical is provided in my laboratory	Strongly agree	42%
	Agree	34%
	Neutral	24%
	Disagree	0%
	Strongly disagree	0%

Table 5 shows the practice of the laboratory staff on personal protective equipment (PPE) and emergency response plan. Regarding personal protective equipment (PPE), 82% of the respondents agreed that PPE is provided in their laboratory in good condition (84 %). The majority of the respondents (86%) claimed that they used proper PPE when performing laboratory work, while 10% were unsure of it and 4 % did not use appropriate PPE. The laboratory staff must wear appropriate PPE while working in the laboratory as it could help to minimize exposure to hazardous chemicals and materials. However, PPE training should be given to the laboratory staff, which covers the proper use of PPE that could help protect the health and safety of the laboratory staff. In terms of the emergency response plan, only 80 % of the laboratory staff revealed that they know the proper emergency response procedures for accidents or injuries in the laboratory. While 86 % of the respondents state that they know the locations and operating procedures for all safety equipment. It is necessary to ensure that all laboratory staff is aware of the proper emergency response. They need to be able to respond to emergencies in the workplace in a competent and speedy manner. Thus, the laboratory management must prepare an emergency response plan and train the laboratory staff to respond if an emergency arises in the laboratory.

Table 5: PPE and emergency response

Category	Sub-category	Response frequency
PPE is provided in my laboratory	Strongly agree	52%
	Agree	30%
	Neutral	16%
	Disagree	2%
	Strongly disagree	0%
PPE provided in a good condition	Strongly agree	53%
	Agree	31%
	Neutral	12%
	Disagree	4%
	Strongly disagree	0%
I use proper PPE when performing laboratory work	Strongly agree	50%
	Agree	36%
	Neutral	10%
	Disagree	2%
	Strongly disagree	2%
I know the proper emergency response procedures for accidents or injuries in the laboratory	Strongly agree	34%
	Agree	46%
	Neutral	18%
	Disagree	2%
	Strongly disagree	0%
I know the locations and operating procedures for all safety equipment (eg: the eyewash station and safety shower)	Strongly agree	54%
	Agree	32%
	Neutral	14%
	Disagree	0%
	Strongly disagree	0%

4. CONCLUSION

The safety practices among laboratory staff focusing on waste disposal are satisfactory. However, the safety practices among laboratory staff could be further improved by ensuring all laboratory staff attends safety training to create a safe environment in the laboratory. Furthermore, a safety model comprising safety culture and practices should be implemented with the support from organizational commitment to ensure a safe workspace in the laboratory. The academic laboratory should also plan and work towards an online database platform that is in line with Industry 4.0 (IR 4.0)

ACKNOWLEDGEMENTS

The authors wish to express their gratitude to Universiti Teknologi MARA Cawangan Pulau Pinang for the technical assistance and financial support provided through the internal research grant 600-TNCPI 5/3/DDN (07) (001/2020), necessary for the completion of this study.

5. REFERENCES

1. H. R. Ayi and C. Y. Hon, “Safety culture and safety compliance in academic laboratories: A Canadian perspective,” *J. Chem. Heal. Saf.*, vol. 25, no. 6, pp. 6–12, 2018, doi: 10.1016/j.jchas.2018.05.002.
2. I. Schröder, D. Y. Q. Huang, O. Ellis, J. H. Gibson, and N. L. Wayne, “Laboratory safety attitudes and practices: A comparison of academic, government, and industry researchers,” *J. Chem. Heal. Saf.*, vol. 23, no. 1, pp. 12–23, 2016, doi: 10.1016/j.jchas.2015.03.001.
3. M. A. Salazar-Escoboza, J. F. Laborin-Alvarez, C. R. Alvarez-Chavez, L. Noriega-Orozco, and C. Borbon-Morales, “Safety climate perceived by users of academic laboratories in higher education institutes,” *Saf. Sci.*, vol. 121, no. September 2019, pp. 93–99, 2020, doi: 10.1016/j.ssci.2019.09.003.
4. B. D. Backus *et al.*, “Laboratory safety culture: Summary of the chemical education research and practice - Safety in chemistry education panel discussion at the 46th Midwest and 39th Great Lakes Joint Regional American Chemical Society Meeting, St. Louis, Missouri, on October ,” *J. Chem. Heal. Saf.*, vol. 19, no. 4, pp. 20–24, 2012, doi: 10.1016/j.jchas.2012.02.001.
5. A. D. Ménard and J. F. Trant, “A review and critique of academic lab safety research,” *Nat. Chem.*, vol. 12, no. 1, pp. 17–25, 2020, doi: 10.1038/s41557-019-0375-x.
6. E. Ramírez Lara *et al.*, “A comprehensive hazardous waste management program in a Chemistry School at a Mexican university,” *J. Clean. Prod.*, vol. 142, pp. 1486–1491, Jan. 2017, doi: 10.1016/j.jclepro.2016.11.158.
7. C. C. Ho and M. S. Chen, “Risk assessment and quality improvement of liquid waste management in Taiwan University chemical laboratories,” *Waste Manag.*, vol. 71, pp. 578–588, 2018, doi: 10.1016/j.wasman.2017.09.029.
8. M. K. Payne, A. W. Nelson, W. R. Humphrey, and C. M. Straut, “The Chemical Management System (CMS): A Useful Tool for Inventory Management,” *J. Chem. Educ.*, vol. 97, no. 7, pp. 1795–1798, 2020, doi: 10.1021/acs.jchemed.9b00905.

AUTOMATED MEASUREMENT OF SCREW THREAD USING MACHINE VISION WITH SUB-PIXEL EDGE DETECTION

Lim Teong Yeong[1], Chiang Ee Pin[2]
[1*,2] *Fakulti Kejuruteraan Mekanikal, Universiti Teknologi MARA, Cawangan Pulau Pinang, Kampus Permatang Pauh, 13500 Permatang Pauh, Pulau Pinang, MALAYSIA.*
(E-mail: tylim527@uitm.edu.my, chiang738@uitm.edu.my)

ABSTRACT- Production of threaded parts in today's industry requires high precision thread metrology. The traditional method of assessing the thread such as thread micrometer and screw pitch gages are considered subjective and less efficient in terms of inspection time. Thus, there is a need to implement an automated inspection system using machine vision (MV) to assess the mass quantity of threads to the highest accuracy. Thread parameters such as thread length, pitch, pitch diameter, minor diameter and major diameter were measured automatically and the screw thread profile was extracted from the scanned images using the sub-pixel edge detection. The resultant measurement was compared to the existing methods using profile projector. The output of this work is beneficial to the quality inspection of thread manufacturing industry.

Keywords: Machine vision, Image Processing, Object detection, Thread measurement, Automated Inspection

1. INTRODUCTION

The traditional method of contact screw measurement and profile projector is unreliable and slow as they require high setup time and varying apparatus for each of the thread parameters to be measured. These traditional processes of thread measurement are inefficient in terms of inspection time due to the tedious and repetitive human labor engagement. There is a need for a precise measurement system in the quality assurance process of the manufacturing industry. Thus, the current MV system can be used in real-time measurement process to achieve accurate and faster results. The MV can be used in automatic quality inspection in terms of technological innovations and image processing algorithms. The technology in this case is the acquisition of the image through image acquisition devices and with the use of suitable algorithms, parameters can be extracted from the image. The features and data extracted are then presented in a way that the inspector can easily comprehend, an interactive Graphical User Interface (GUI). In the manufacturing of screw threads, the standard parameters to observe is the major diameter, minor diameter, pitch diameter, pitch and thread length in accordance to ISO standard. In this paper, the MV method was compared to the conventional manual profile projector to evaluate their differences in terms of measurement accuracy. Sub-pixel edge detection was developed to allocate the object edge in order to increase the precision of detection.

2. BACKGROUND OF RESEARCH

Screw thread profile is the helical structure on the screw that ensure mating with the complementary thread. The most commonly used thread profile standard is the ISO metric screw standard (ISO 68,

IS 4218-1976). Some other standards commonly adopted are the Unified Thread Standard in America and Canada and the British Standard Whitworth. In ISO metric standard, the important parameters used are Major, Minor, Length, Pitch and Pitch Diameter. The ISO metric profile is also written in order to address these parameters as shown in Figure 1. These parameters are important in the study to extract the relevant parameters as derived in the standard.

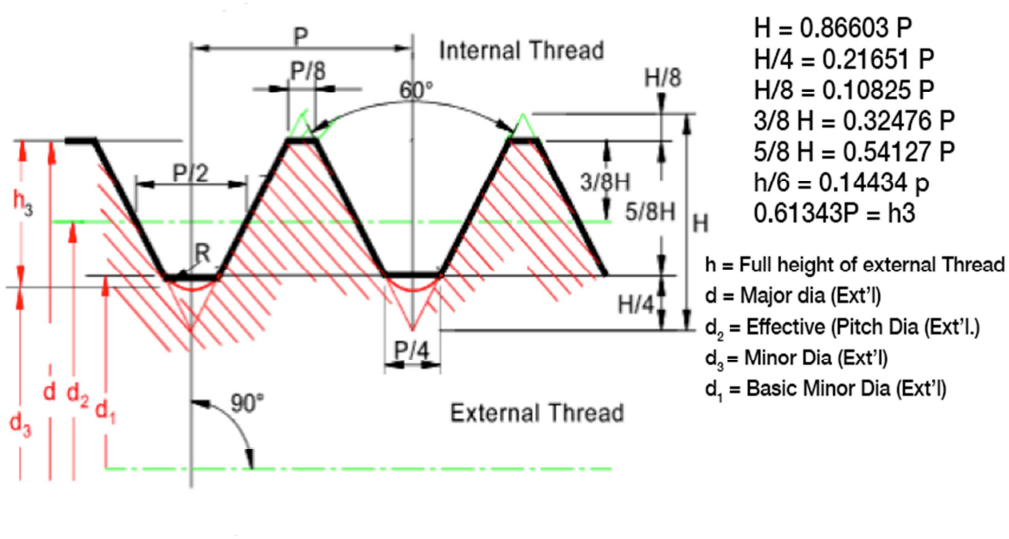

Figure 1: ISO thread form.

The MV with the integration of computer algorithms is fast and accurate method with the option of automation [1] where less human involvement is preferred. The non-contact and non-intrusive method is an attribute of the MV inspection system. This method also has a convenience to be automated as it is integrated between hardware and software. The whole process from feature recognition, measurement and the standard comparison can be automated. This speed up the whole process over traditional methods and has proven to be stable and accurate [1]. The MV is also applied in a wide field of practice in object recognition, for instance, the detection of damages in beams [2], measuring a cutting insert's parameters [3] and [4-5], manufacturing processes [6-7] applications in agriculture such as inspection of starfruits [8], eggs quality [9] and vegetables recognition [10].

Sub-pixel edge detection in image processing is concerned with determining precise location of an edge within pixels [11]. In image processing, the sub-pixel accuracy refers to the sub-pixel resolution that can be obtained beyond its nominal pixel resolution by defining lines, points or edges using algorithm that can reliably measure the precise location of the edge.

3. METHODOLOGY

The measurement process of screw thread in this research was separated into two parts which are MV (automated and non-automated) and manual inspection using profile projector.

3.1 Image Acquisition and Processing

The image processing and edge detection algorithms flow for thread image captured are shown in Figure 2. The algorithm starts from image preprocessing (filtering), followed by a simple thresholding. Then, the original image was subjected to morphological dilation and erosion separately to obtained their corresponding subtraction image. Multiplication of images was applied between the subtracted image and the original filtered image. Then, subpixel edge detection was taking place to obtain the object edges. Finally, features were extracted from the edges and parameters were obtained.

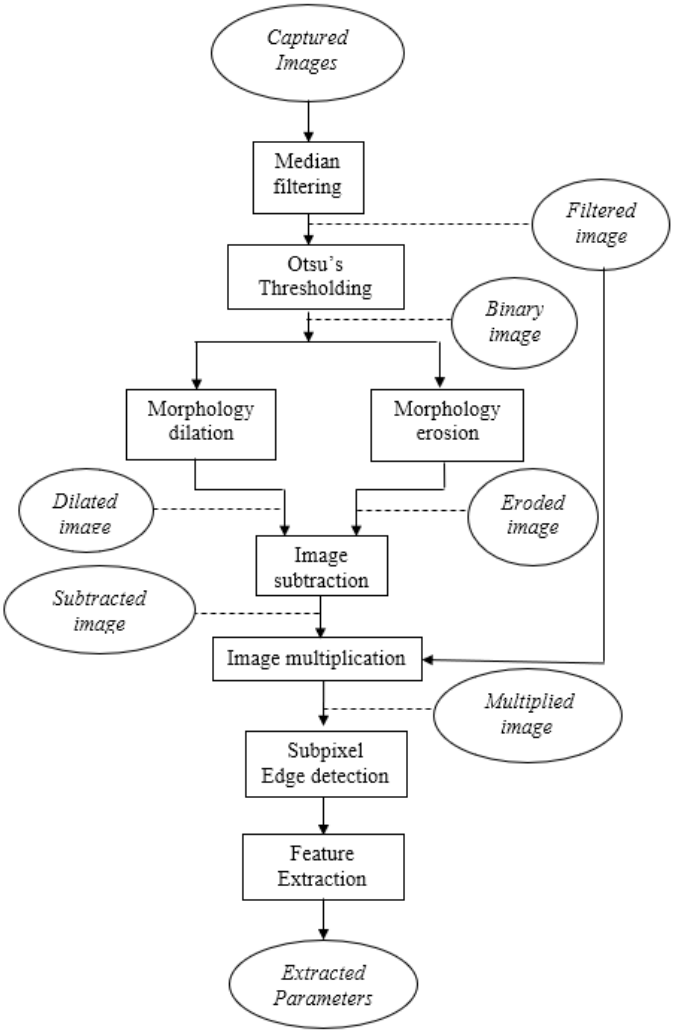

Figure 2: Flowchart of image processing algorithms

In the measurement of screw threads using machine vison the process is divided into three sections namely the experimental setup, the software implementation and the algorithms development. The image acquisition used in this research is a Charge-coupled Device (CCD) camera (Sony EC-ES50) to acquire the images of screws and the software used was MATLAB® image analysis tools to extract the required features and to measure them in accordance to the designated parameters. The

algorithms were developed according to ISO parameters. Sample images captured are shown in Figure 3. These images were processed using image processing and feature extraction algorithms. The parameters calculated are thread length, pitch, pitch diameter, minor diameter and major diameter. The images captured were used to extract the parameters visually (manual MV) as well as automatically (automatic MV). Measurement results are then compared with the traditional method using profile projector.

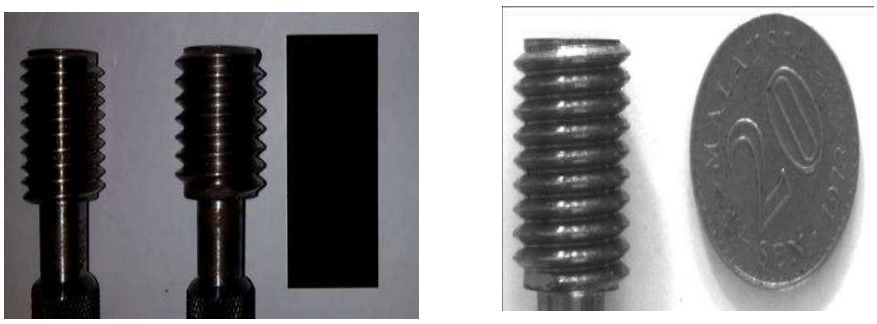

Figure 3: Sample images used for algorithm development

3.2 Feature Extraction: Peak, Root and Pitch

To measure the major, minor and pitch from the screw thread images, peak, root and pitch were extracted using the algorithms as shown in Figure 4.

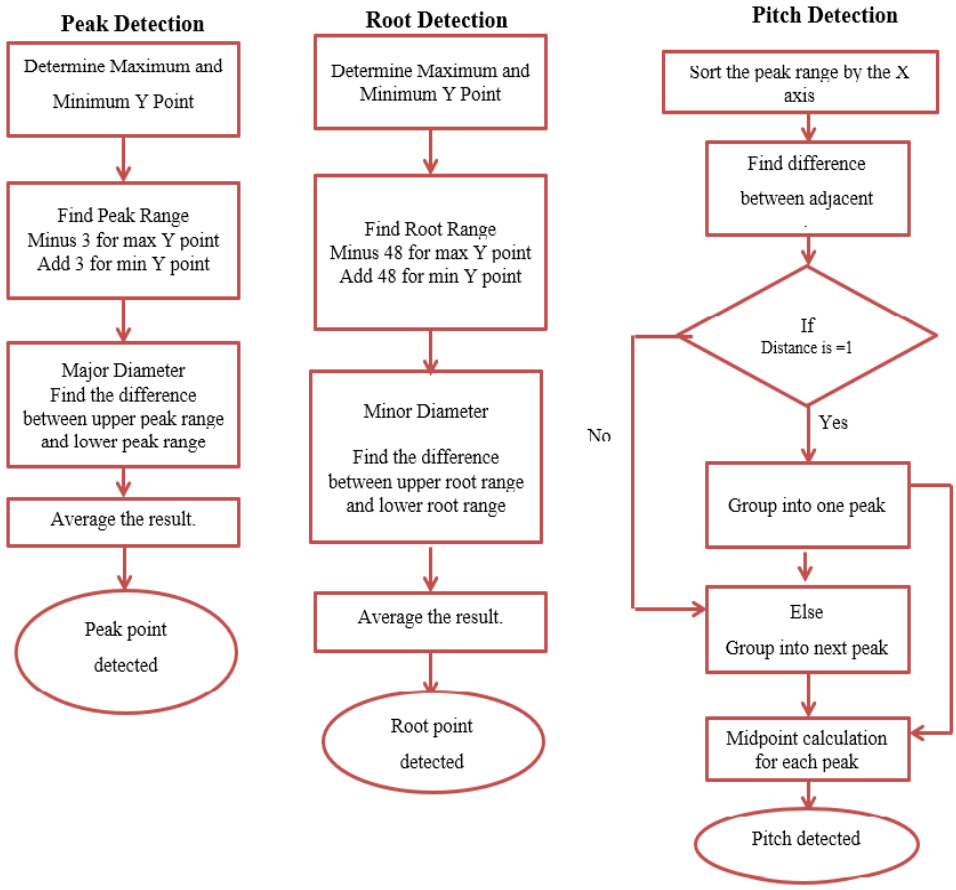

Figure 4: Flowchart of peak, root and pitch extraction.

The peaks and roots are divided into upper and lower section. This corresponds to the upper and lower region of the screw thread. Since both of this section is identical in terms of shape, the same algorithm can be applied for both of them. The peak algorithm is used to find the upper peaks and lower peaks, while the root algorithm is used to find the upper root and lower root. It is found that the maximum minimum of y coordinates are always the peak points. However, we must also consider the object tilting (orientation) as it changes the peak y coordinate value. This can be solved by adding a range of possible peak points. By extending five pixels from the maximum and minimum y coordinates, we can include most of the peaks with this range. Using the concept from the peak algorithm, instead of directly using the max and min y coordinates, the algorithms use a point of 48 pixels away from the max and min y point to get to the root points. From this point, a range of six pixels is used to calculate all the possible root value.

Pitch, on the other hand is a different measurement compared to minor and major diameter. It is a measure of distance between the adjacent peak points and not corresponds to the upper and lower points. Thus, the peak range acquired from the peak algorithm was sorted by the x axis. Then the algorithm will sort them into individual peaks. These individual peaks have an array of points and to calculate the pitch, it only requires one point; thus, a midpoint is calculated for every peak. Finally, the distance between the midpoint is pitch value.

3.3 Conventional Measurement

The second part of the research was the collection of measurement data using traditional measurement method which is the profile projector. The measurement data was then compared with the proposed method to determine the difference in terms of measurement. For comparison purpose, the manual inspection of screw thread using conventional profile projector was conducted. The machine model is ST 3550-20-3500 made by the Scheer Tumico S-T Industries , Inc. Figure 5 shows a 14' Horizontal Beam Optical Comparator.

Figure 5**:** The 14' Horizontal Beam Comparator.

4. RESULTS AND DISCUSSIONS

The results for manual vision measurement are shown in Figure 6. For instance, the peak-to-peak and the major diameter parameters were determined by estimating the points using cursor. The results were generated automatically by the MATLAB Image Utility. On the other hand, the feature extraction results were obtained by automatic feature extraction algorithm developed which extracts the peaks and roots of each thread as shown in Figure 7.

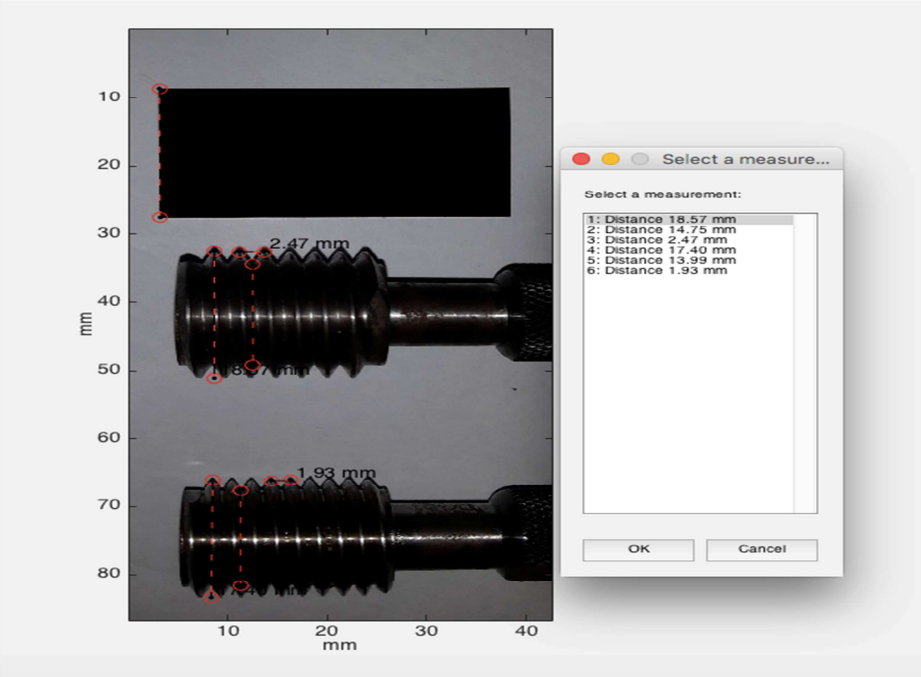

Figure 6: Results of Image Measurement Utility for Screw M18.

The features were then used to calculate the major, minor diameter and pitch of the threads. The corner point consists mostly of the peaks and the root. The algorithms detect the peaks and roots and to assume that the four most common corner points are: upper peak, upper root, lower peak and lower root as shown in Figure 8.

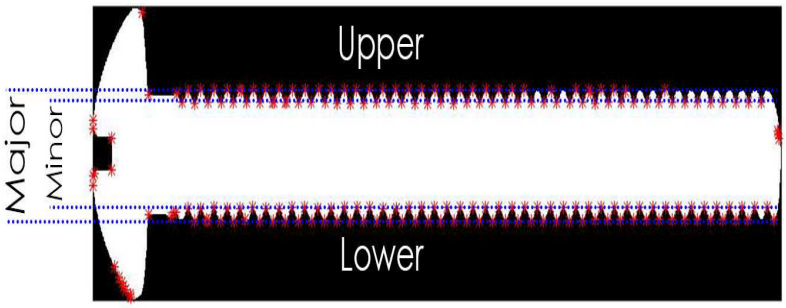

Figure 7: The diagram shows the upper and lower section of the screw.

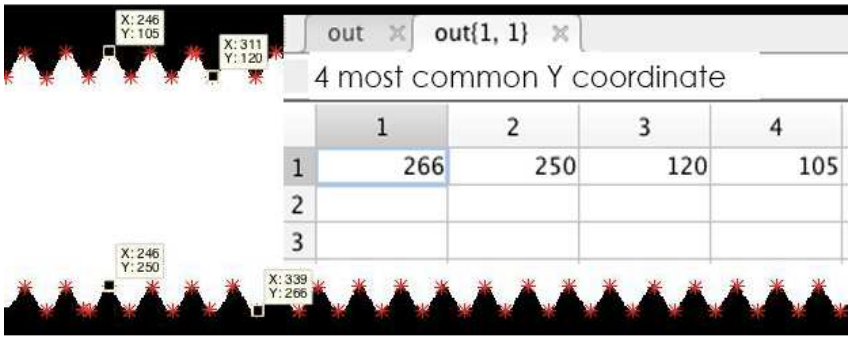

Figure 8: The 4 most common points obtained is the same as the Y coordinates of the peaks and root

Table 1 and Table 2 shows the results obtained from the manual MV method, automatic MV method and the conventional method using M16 and M18 threads. From the results obtained, it is obvious that the manual inspection using MV yields a difference smaller than 5% whereas comparatively higher difference was found using automatic detection. Highest difference of about 8% were found for automatic detection. This may be due to the algortihms developed were not able to detect the object with lower background contrast and shadows. However the close measurement between both methods (MV) with the conventional method using profile projector, show a preferance in using MV since the measurement using profile projector requires high labor attention and equipement calibration.

During the image acquisition, shadows were produced, as well as the light relective region, as shown in Figure 9. This indirectly affects the accuracy of the automatic method during the binarization and subpixel edge detection stages. The shadow appearance however will not affect the manual MV method as it requires the user to judge the edges of the object, which the use can easily distinguish between a shadow and an object. From the results of measuring major and minor diameter, it is found that generally higher absolute difference were found for minor diameter of thread. This agrees with the results of image measurement screw thread by compensation of thread profile by Chen [12] to encounter the problem of distortion especially in minor diameter.

Table 1: Results obtained for M18 screw thread

M18	Auto MV /mm	Manual MV /mm	Conventional /mm	Absolute difference /%	
				Auto MV VS conventional	Manual MV VS conventional
Major Diam.	18.914	18.570	18.013	5.00	3.09
Minor Diam.	15.635	14.950	14.392	8.63	3.88
Pitch	2.508	2.470	2.496	0.48	1.04

Table 2: Results obtained for M16 screw thread.

M18	Auto MV /mm	Manual MV /mm	Conventional /mm	Absolute difference /%	
				Auto MV vs conventional	Manual MV VS conventional
Major Diam.	16.268	16.150	16.020	1.55	0.81
Minor Diam.	13.566	13.360	13.064	3.84	2.27
Pitch	2.018	1.960	2.003	0.75	2.15

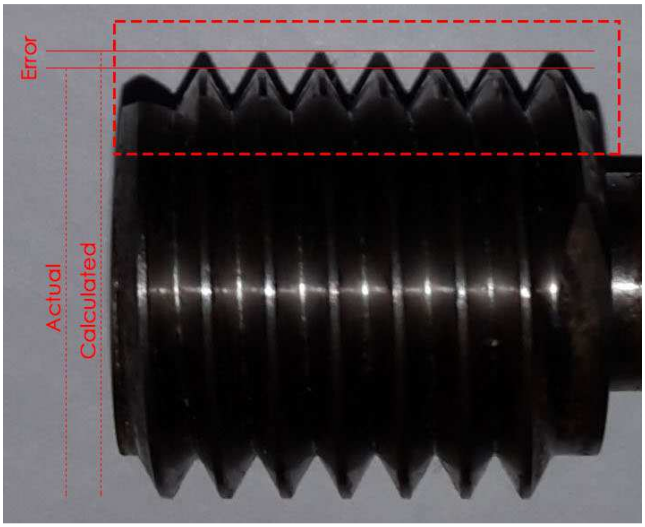

Figure 9: The image acquired with shadows and reelection

5.0 CONCLUSIONS

The proposed method of screw thread measurement using the MV can reduce the time of inspection and increase the accuracy of measurement. About 5% to 8% difference were found between the manual method and the machine vision method. The next phase of the research is to compare the measurement results with high-end metrology system such as variable focus metrology imaging system to analyze the errors occurred in the proposed methods.

ACKNOWLEDGMENT

The authors would like to express gratitude for the support given by the Universiti Teknologi MARA.

5. REFERENCES

1. R. J. Hunsicker, P. John, L. Alton, F. Cathie, A. Michael, and E. Clark, Automatic vision inspection and measurement system for external screw threads, *Journal of Manufacturing Systems*, vol. 13, no. 5, pp. 370–384, 1994.
2. J. Shi, S. Jing, X. Xiangjun, W. Jialai, and L. Gong, Beam damage detection using computer vision technology, *NDT&E International*, vol. 25, no. 3, pp. 189–204, 2010.
3. T.Y.Lim and M. M. Ratnam, Measurement of nose radii of multiple cutting tool inserts from scanned images using sub-pixel edge detection, in *Proc. 13th International Conference on Control Automation Robotics & Vision (ICARCV)*, 2014.
4. D. H. Ballard, Model-directed Detection of Ribs in Chest Radiographs. Ph.D. dissertation. University of Rochester, 1978.
5. B. Madhulika, Y. Divakar, Madhurima, G. Pritee, K. Gurpreet, S. Jyoti, G. Mallika, and S. Ajeet, Implementing Edge Detection for Medical Diagnosis of a Bone in Matlab, in *Proc. 5th International Conference on Computational Intelligence and Communication Networks*, 2013.
6. W.Dai, D, Li, Q. Jiang, D. Wang, H. Wang, Y Peng. Deep Learning assisted vision inspection of resistance weld spots, *Journal of Manufacturing Processes*, vol.62, pp.262-274, 2021.
7. A. Akundi, M.Reyna, A Machine vision based quality inspection system for product dimensional analysis, *Procedia Computer Science*, Vol.185, pp127-134, 2021.
8. M. Z. Abdullah, A. S. Fathinul-Syahir, and B. M. N. Mohd-Azemi, Automated inspection system for colour and shape grading of starfruit (Averrhoa carambola L.) using machine vision sensor, *Transactions of the Institute of Measurement and Control*, vol. 27, no. 2, pp. 65–87, 2005.
9. A. S. Alon, R.I. Marasigan, Jr., J.G. Nicolas- Mindoro C.D. Casuat, An Image Processing Approach of Multiple Eggs' *Quality Inspection, International Journal of Advanced Trends in Computer Science and Engineering*, vol. 8, no.6, pp2794-2799, 2019.
10. N.A. Nasharuddin, N.S.M Yusoff, S. K. Ali, Multi-feature Vegetable Recognition using Machine Learning Approach on Leaf Images, *International Journal of Advanced Trends in Computer Science and Engineering*, vol. 6, no.4, pp. 1789-1794, 2019.
11. X. Wang, Xiaojia, G. Jun, and W. Lei, A survey of subpixel object localization for image measurement, in *Proc International Conference on Information Acquisition , 2004.*
12. M. Chen, Compensation of thread profile distortion in image measuring screw thread, *Measurement*, vol. 129, pp. 582-587, 2018.

FORMATION OF ECO-FRIENDLY CHARCOAL BY A LOW COST METHOD

Iqbal Zharfan Masrul Hasdi[1], Mohamad Dzulhisyam Dzulkifli[1], Muhammad Aliff Daniel Mansor[1], Muhammad Azri Khir Mohd Zokeri[1], Muhammad Danial Azeem Muhammad Dzahir[1], Noorsalawati Ahmad[1]; Noraini Mohd Ismail[1], Mohd Zaki Mohd Yusoff[2], Muhammad Firdaus Othman[3], Mohd Bukhari Md Yunus[2]

[1]Sultan Mohamad Jiwa Science Secondary School, Jalan Badlishah, 08000 Sungai Petani,Kedah Darul Aman
smssmj.ppdkmy@gmail

[2]Department of Applied Sciences, Universiti Teknologi MARA (UiTM) Cawangan Pulau Pinang, 13500 Permatang Pauh, Pulau Pinang, Malaysia.*
zaki7231@uitm.edu.my

[3]Faculty of Applied Science, Universiti Teknologi MARA, Cawangan Pahang, 26400 Bandar Tun Abdul Razak Jengka, Pahang, Malaysia
firdaus327@uitm.edu.my

[2]Department of Applied Sciences, Universiti Teknologi MARA (UiTM) Cawangan Pulau Pinang, 13500 Permatang Pauh, Pulau Pinang, Malaysia.
bukhari.myunus@uitm.edu.my

ABSTRACT- Charcoal applications in everday life, such as a fuel for combustion, have piqued people's interest. Commercial charcoal on the other hand, is typically produced by cutting down mangrove trees, which is not sustainable and reduces the natural barrier against erosion, storms, and floods. Hence, a new eco-friendly homemade charcoal was produced to replace the commercial charcoal. The new processed charcoal material was produced by two-step conventional pyrolysis methods involving daily waste materials such as orange peels, banana peels and paddy husk. The scanning electron microscopy (SEM) images showed that the number of air pores in the processed sample is higher compared to the commercial charcoal. Samples with higher air pore numbers are believed to produce more ignition due to the higher oxygen levels around the sample. The energy dispersive X-Ray spectroscopy (EDS) results indicated higher ignition elements in the processed sample compared with the commercial sample.

Keywords: Activated Carbon, Charcoal, Banana Peels, agricultural waste.

1. INTRODUCTION

The deforestation of mangrove trees for producing commercial charcoal reveals the instability of the ecosystem and causes the water-flooded. Eco-friendly charcoal is believed to be an alternative to wood fuel and successfully reduced deforestation activity. Using agricultural waste as the main raw material, eco-friendly charcoal is believed to give a positive impact on the environment and avoiding mangrove tree elimination. The mixed agricultural waste is carbonized using a homemade pyrolysis system and then crushed and held together with a binder and formed into briquettes. These briquettes are more efficient and eco-friendly compared to commercial charcoals. The objective of this work is to fabricate eco-friendly charcoal using agricultural waste materials. Orange peels, banana peels and paddy husk are chosen as potential

agricultural waste to produce eco-friendly charcoal. Orange peels contain a porous structure and have the property of a hydrophilic surface [1], which identifies as a low-cost adsorbent [2]. Meanwhile, banana peels are a solid waste from finished food products, such as chips, slices, and dried bananas. They are high in organic carbon (41.37%) [3]. This waste has been subjected to bio methanation [4] and biogas production [5]. Paddy husk has contributed to 20-30% as waste material from the rice mills [6]. Paddy husk contains an element of cellulose, hemicellulose and lignin [7]. Surface morphology and existed elements were characterized by energy-dispersive X-ray Spectroscopy (EDS), Scanning Electron Microscope (SEM). The air pores area formed within the samples were illustrated by Image processing, Image J software.

2. EXPERIMENTAL DETAILS

Orange peels, banana peels, paddy husk, sand were collected as wastes from the local fruit markets in Sungai Petani, Malaysia. All samples were cleaned with water to remove surface dirt. The orange peels, banana peels, paddy husk and sand were mixed based on the ratio as stated in Table 1. The mixed samples were then carbonized using a homemade pyrolysis system (refer to step 4 in Figure 1). Finally, the samples were dried again at room temperature for several minutes before the characterization process was conducted.

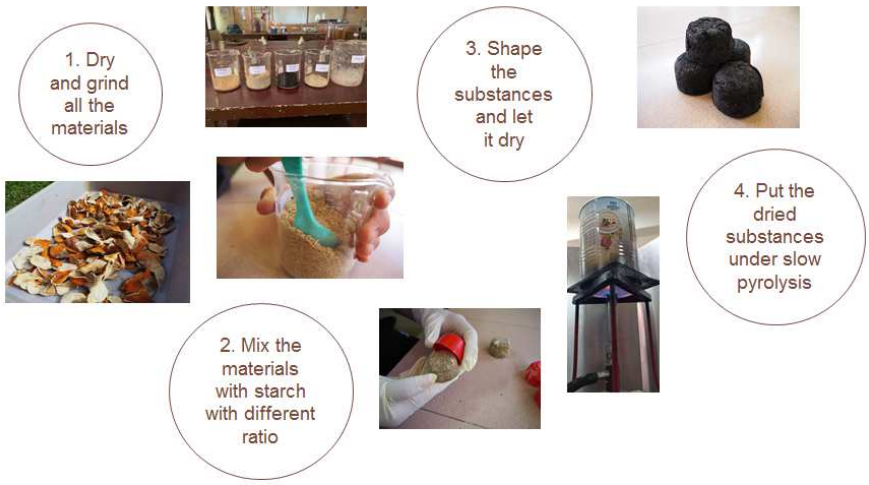

Figure 1: Steps to prepare homemade charcoals using an agricultural waste

Table 1: Samples with different masses of agricultural wastes

Samples	Mass of Substances (g)			
	Orange Peels	Banana Peels	Paddy Husk	Sand
1	15	15	15	5
2	15	10	20	5
3	15	20	10	5
4	20	15	10	5

3. RESULTS AND DISCUSSION

Figure 2 (a)-(d) shows the surface morphology of the mixed charcoals fabricated at different wastes compositions. It shows that the structure of all samples is highly porous compared to the control sample (Figure 2 (e)). Due to the low-density area of the sample, they have issues with sample handling and mechanical characteristics [8]. While, the porous shapes of mixed charcoals offer particle capillary binding and surface mechanical interlocking [9]. The air pores of samples were determined by Image processing, Image J software, as shown in Figure 3. Sample 2 (1868) indicates the highest air cavity reading, followed by sample 4 (1767), sample 3 (1557), sample 1 (1397), and control (560). Generally, all the mixed samples had small and low volume pores compared to the commercial sample. Interestingly, samples with higher air pore readings will result in a higher combustion rate from the burning activity due to more exposed surface areas and the higher oxygen level. The efficiency of the combustion process will be determined by the rate of burning i.e. the burning rate of fuel has an impact on the delivered energy [10]. The higher air pores formed thus results in a higher burning rate. Therefore, it is found that sample 2 has a higher combustion rate compared to other samples.

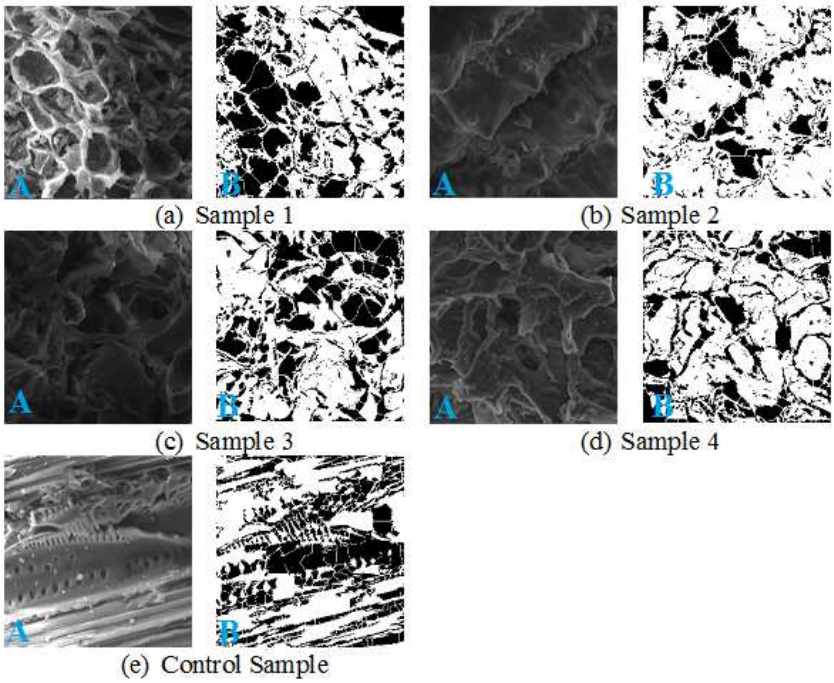

Figure 2 (a)-(e): SEM morphology of mixed charcoals before (A) and after (B) treatment by ImageJ for determination of the air pores (black area)

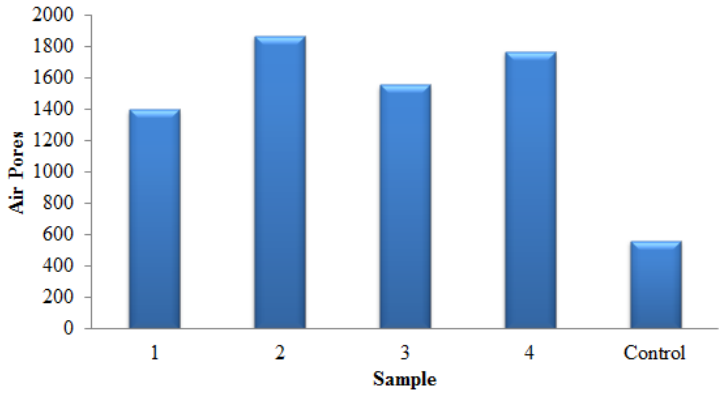

Figure 3: Samples with different number of air pores

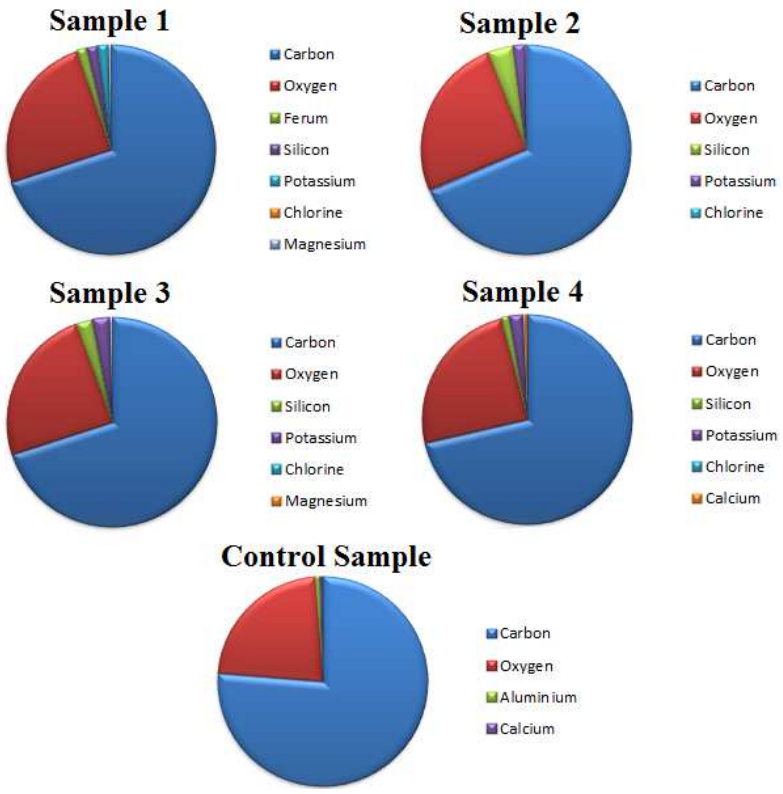

Figure 4: EDS analysis on mixed charcoal samples

Figure 4 shows the EDS analysis on mixed charcoal samples. No contamination and heavy metals were detected from the samples. All samples showed a higher percentage of carbon (C) and oxygen (O).

4. CONCLUSION

Eco-friendly charcoal was successfully grown at a different agricultural waste ratio. Orange peels, banana peels and paddy husk were identified as potential agricultural waste to produce eco-friendly charcoal. SEM images showed a small and low-density area of air pores for the mixed charcoal samples. Higher air pore samples indicated a higher burning rate compared to the commercial sample. The energy dispersive X-Ray spectroscopy (EDS) results indicated higher ignition elements in the processed sample compared with the commercial sample.

ACKNOWLEDGEMENTS

The authors would like to express gratitude for the support given by the Sultan Mohamad Jiwa Science Secondary School and Universiti Teknologi MARA.

5. REFERENCES

1. M. C. Mittelmeijer-Hazeleger, and J. M. Martin-Martinez. Carbon 30.4 (1992) 695-709.
2. Xie, Z., Guan, W., Ji, F., Song, Z., & Zhao, Y. Journal of Chemistry, (2014) 2014.
3. Mopoung, S., Journal of Microscopy Society of Thailand, 22, (2008) 15-19.
4. N. Bardiya, D. Somayaji, & S. Khanna, Bioresource technology, 58(1), (1996) 73-76.
5. Mopoung, S., Udeye, V., Mopoung, R., Boonphong, S., O. Donnohuy, J., Nation. Res. Counc. Thail. 2000, 432, 23-28.
6. S. Dani Maulida, and F. Bukhori, Int. J. of Science and Research 4, (2015) 2146-2148
7. S. Suryaningsih, O. Nurhilal, Y. Yuliah, & E. Salsabila, AIP Conference proceedings 1927 (2018) 030044
8. W.B. Kusumaningrum, and S.S. Munawar, Energy Procedia, 47: (2014) 303-309.
9. A. Bazargan, S.L. Rough and G. McKay, Biomass Bioenergy, 70: (2014) 489-497.
10. Y. Huangfu, H. Li, X. Chen, C. Xue, C. Chen, & G. Liu, Energy for Sustainable Development, 21, (2014) 60-65.

TENSILE STRENGTH OF TIG WELDED ULTRAFINE-GRAINED 5083 AL ALLOY JOINTS

Ahmad Farrahnoor[1*], Muhammad Haziq Mohd Asri[1] and Anasyida Abu Seman[2]
[1] *Faculty of Mechanical Engineering, Universiti Teknologi MARA, Cawangan Pulau Pinang, Kampus Permatang Pauh, Permatang Pauh, Penang, MALAYSIA.*
[2] *School of Materials and Mineral Resources Engineering, Universiti Sains Malaysia, Engineering Campus, Nibong Tebal, Penang, MALAYSIA.*
(E-mail: farra728@uitm.edu.my)

ABSTRACT- Being a lightweight metal, 5083 aluminum alloy is used to replace steels in automotive industry. Although tungsten inert gas (TIG) welding is ideally suited for joining 5083 aluminum alloy, some key issues are however present with the welding of ultrafine-grained aluminum as a result of thermal cycle during welding. This research work aims to investigate the effect of varying welding currents (70 A, 80 A, 90 A, and 100 A) on the mechanical properties of ultrafine-grained 5083 aluminum alloy using TIG. The tensile properties of the butt weld joints were determined using a universal tensile testing machine in accordance with ASTM E8. The experimental results disclosed that with increasing welding current to 90 A, the tensile strength of the cryo-rolled samples reached its optimum at 106.99 MPa, as a result of more plastic deformation and stronger metallurgical connections at the joint contact. However, a further increase in the welding current to 100 A had resulted in decreasing tensile strength of 78.68 MPa. This is because the depth of weld penetration at excessive welding current tends to melt the weld through the joining metal, thus forming hotspots and declining the tensile strength. Ultimately, the study revealed that the tensile strength of ultrafine-grained 5083 aluminum alloy is significantly dependent on welding current.

Keywords: Tungsten inert gas, Tensile strength, Welding current, Aluminum alloy, Cryorolling

1. INTRODUCTION

5083 aluminum alloy is widely used in automotive body panels, car structural parts and car chassis owing to its lightweight, high resistance to corrosion to boost fuel consumption efficiency, and low emission of carbon [1],[2]. A further enhancement in the tensile strength of 5083 aluminum alloy can be achieved via cryo-rolling process which utilizes strain hardening to produce ultrafine-grained materials of grain sizes below 1 µm [3].

Cryo-rolling is a rolling method for producing metals of ultrafine-grained structure using liquid nitrogen at a low temperature (77 K) [4]. In this process, the fabricated material cools to room temperature and its molecular structure contracts, resulting into supersaturated solid solution. Therefore, the cryo-rolling method could greatly improve the mechanical properties of a material due to less plastic deformation in comparison to other severe plastic deformation processes at important temperatures.

The application of cryo-rolling on aluminum alloy has received limited attention worldwide. Since thermal cycle plays a great role in a welding process, the determination of optimum welding current is crucial for better weldment of joints through lack of fusion prevention. It is more critical in the welding of 5083 aluminum alloys, which are sensitive to the heat input causing the porosity formation and solidification cracking [5]. Therefore, the welding current must be properly adjusted to achieve good heat input. In the current study, tensile test was utilized to investigate the mechanical properties of cryo-rolled 5083 aluminum alloy subjected to various welding currents.

2. EXPERIMENTAL DETAILS

Ultrafine-grained 5083 Al alloy of 2.9 mm thickness was prepared by cryo-rolling with as-received 5083 Al alloy of 3 mm thickness as the reference material, as shown in Figure 1. Acetone solution was used to clean the sample surface from oil, grease, and corrosive substances. The dimensions of the samples were of 50 mm length and 20 mm width. Prior cryo-rolling process, sample was pre-annealed at 300 °C for 2 hours. Then, the sample was dipped in liquid nitrogen at an extremely low temperature which is between -210.2 °C and -196.0 °C for 60 min followed by cryo-rolled to 30% reduction in thickness.

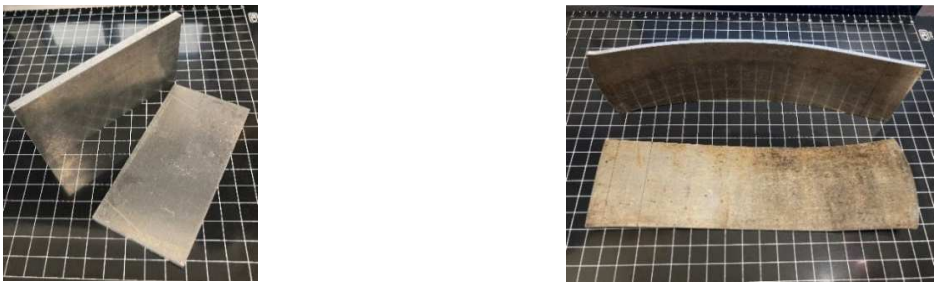

(a) (b)

Figure 1 : (a) As-received 5083 Al alloy and (b) Ultrafine-grained 5083 Al alloy

The aluminum plates are placed on the welding table where the welding process is carried out. The sample was clamped on a custom fixture using curve jaw locking pliers for stable welding positioning, as shown in Figure 2. TIG welding (SUPERTIG 180 AC/DC) with ER 5356 filler rod (1.6 mm) made of aluminum, as well as gas nozzle of size 6 (3/8 inch) were utilized in this research work. Moreover, varying welding currents of 70 A, 80 A, 90 A, and 100 A were investigated at constant gas flow of 5 liter/min. The post flow for the gas shielding was set at 3 sec.

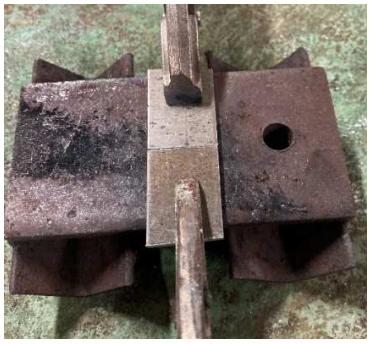

Figure 2 : Sample preparation for welding process

Tensile test was carried out using AG-IS SHIMADZU instrument at ambient temperature and cross-head speed of 1 mm/min, in accordance to the ASTM E8 standard. Duplicate tests were considered for each tensile test to ensure data reproducibility. From this test, the ultimate tensile stress (UTS) was determined from the stress-strain data.

3. RESULTS AND DISCUSSION

The tensile strength of as-received 5083 Al alloy and ultrafine-grained 5083 Al alloy is shown in Figure 3. A gradual increase in tensile strength was observed in the latter with increasing welding current for ultrafine-grained 5083 Al alloy. However, at 100 A, its strength had suddenly dropped to 78.68 MPa. On the other hand, the as-received 5083 Al alloy also demonstrated increasing tensile strength pattern with increasing current at the early stage, but dramatically dropped to 69.61 MPa at 90 A, before again increased to 82.79 MPa at 100 A.

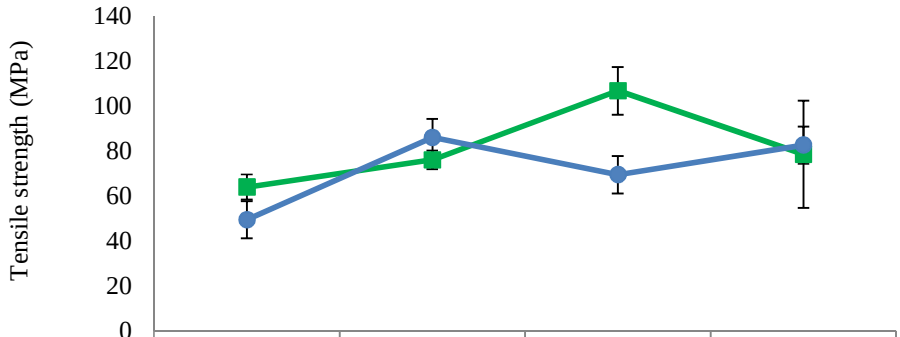

	70 A	80 A	90 A	100 A
Ultrafine-grained 5083 Al alloy	64.02	76.21	106.99	78.68
As-received 5083 Al alloy	49.51	86.17	69.61	82.79

Figure 3 : Tensile strength of ultrafine-grained 5083 Al alloy and as-received 5083 Al alloy at various welding currents

The as-received 5083 Al alloy exhibited the lowest tensile strength of 49.51 MPa and highest tensile strength of 86.17 MPa at welding current of 70 A and 80 A, respectively. The maximum tensile strength (106.99 MPa) and minimum tensile strength (64.02 MPa) of ultrafine-grained 5083 Al alloy were achieved at 70 A and 90 A, respectively.

Generally, both types of Al alloys demonstrated low tensile strength at 70 A welding current due to low heat input. An inadequate heat input may cause uneven melting of filler and parent metal, thus resulting in a less mature and uneven melt. This consequently imposes significant effects on the welding quality with incomplete welding of metal plate and suppressed strength of the joints. For the ultrafine-grained 5083 Al alloy, high welding current yielded high tensile strength due to the excellent fusion between the filler and base metals. Higher current increases the penetration depth which leads to greater melting of base metals, thus increases the tensile strength. Nevertheless, the optimum tensile strength was achieved at 106.99 MPa at a welding current of 90 A.

The variation in the tensile strength of the as-received 5083 Al alloy is due to the change in its microstructure. In general, a weld microstructure consists of a mixture of martensite, austenite, and certain amount of ferrite. Due to excessive current at 100 A, the overheating of base metal has resulted in the production of hotspots and a shift in the phase balance between the ferrite and austenite phases [6]. Hence, the increase in the amount of ferrite in the weld deposit by the enhancement of heat input has resulted in lower strength [7]. When higher current is applied, more welding heat is generated, thus expands the heat affected zone (HAZ) region. Therefore, minimum reduction in the mechanical properties is observed. Meanwhile, regardless of heat input, HAZ near the fusion line comprises of a bigger and more elongated brilliant phase of banded delta ferrite in a matrix of martensite. In another study, Kah et al. [8] reported that a high heat input leads to a lower nucleation and produces coarser grains around the weld interface. This phenomenon contributes to low mechanical properties in a weld. Apart from grain morphologies, the evaporation of magnesium in 5083 Al alloy turned out to be porosity that also affected the joints strength [9].

4. CONCLUSION

The finding of this research work revealed that welding current affects the tensile strength of aluminum alloys. The highest tensile strength achievable by the ultrafine-grained 5083 Al alloy and as-received 5083 Al alloy was 106.99 MPa at 90 A and 86.16 MPa at 80 A, respectively. Indeed, the melting of the parent metal requires an appropriate amount of heat energy that is neither excessive nor insufficient. When sufficient heat is applied to melt the filler metal combined with a good parent metal, a strong welding joint could be formed.

ACKNOWLEDGEMENTS

The authors would like to express their gratitude for the supports provided by Universiti Teknologi MARA (UiTM) and Universiti Sains Malaysia in the accomplishment of this research.

5. REFERENCES

1. A. Hidayat, A. Junaidi, S. Mudiantoro, and W. Winarto, *IOP Conf. Ser. Mater. Sci. Eng.*, vol. 924, no. 1, 2020, 1-11.
2. W. Abuzaid, R. Hawileh, and J. Abdalla, *Infrastructures*, vol. 6, no. 6, 2021, 1–17.
3. Q. Yuan, G. Xu, S. Liu, M. Liu, H. Hu, and G. Li, *Metals (Basel)*, vol. 8, no. 7, 2018, 1-14.

4. Y. C. Huang, X. Y. Yan, and T. Qiu, *Trans. Nonferrous Met. Soc. China (English Ed.)*, vol. 26, no. 1, 2016, 12–18.
5. M. Samiuddin, J. long Li, M. Taimoor, M. N. Siddiqui, S. U. Siddiqui, and J. Tao Xiong, *Def. Technol.*, vol. 17, no. 4, 2021, 1234–1248.
6. A. Ozlati and M. Movahedi, *J. Manuf. Process.*, vol. 35, 2018, 517–525.
7. C. Muthusamy, L. Karuppiah, S. Paulraj, D. Kandasami, and R. Kandhasamy, *Mater. Res.*, vol. 19, no. 3, 2016, 572–579.
8. P. Kah, M. Olabode, E. Hiltunen, and J. Martikainen, *Mechanika*, vol. 19, no. 1, 2013, 96–103.
9. L. Huang, D. Wu, X. Hua, S. Liu, Z. Jiang, F. Li, H. Wang and S. Shi, *J. Manuf. Process.*, vol. 31, 2018, 514–522.